Optimized structures for vibration attenuation and sound control in nature: A review

Optimized structures for vibration attenuation and sound control in Nature: a review

Federico Bosia[1], Vinicius F. Dal Poggetto[2], Antonio S. Gliozzi[1], Gabriele Greco[2], Martin Lott[1], Marco Miniaci[3], Federica Ongaro[2], Miguel Onorato[4], Seyedeh F. Seyyedizadeh[1], Mauro Tortello[1], Nicola M. Pugno[2,5*]

[1] Department of Applied Science and Technology, Politecnico di Torino, Torino, 10129, Italy
[2] Laboratory for Bioinspired, Bionic, Nano, Meta Materials and Mechanics, Department of Civil, Environmental and Mechanical Engineering, University of Trento, Trento, 38123, Italy
[3] CNRS, Univ. Lille, Ecole Centrale, ISEN, Univ. Valenciennes, IEMN - UMR 8520, Lille, F-59000, France
[4] Department of Physics, University of Torino, Torino, 10125, Italy
[5] School of Engineering and Materials Science, Queen Mary University of London, London, E1 4NS, UK

* Corresponding author: nicola.pugno@unitn.it

Summary:

Nature has engineered complex designs to achieve advanced properties and functionalities through millions of years of evolution. Many organisms have adapted to their living environment producing extremely efficient materials and structures exhibiting optimized mechanical, thermal, optical properties, which current technology is often unable to reproduce. These properties are often achieved using hierarchical structures spanning macro, meso, micro, and nanoscales, widely observed in many natural materials like wood, bone, spider silk and sponges. Thus far, bioinspired approaches have been successful in identifying optimized structures in terms of quasi-static mechanical properties, such as strength, toughness, adhesion, but comparatively little work has been done as far as dynamic ones are concerned (e.g. vibration damping, noise insulation, sound amplification, etc.). In particular, relatively limited

knowledge currently exists on how hierarchical structure can play a role in the optimization of natural structures, although concurrent length scales no doubt allow to address multiple frequency ranges. Here, we review the main work that has been done in the field of structural optimization for dynamic mechanical properties, highlighting some common traits and strategies in different biological systems. We also discuss the relevance to bioinspired materials, in particular in the field of phononic crystals and metamaterials, and the potential of exploiting natural designs for technological applications.

1. Introduction

It is well known that engineering materials such as metals or fibre-reinforced plastics are characterized by high stiffness at the expense of toughness. In particular, these materials do not efficiently dissipate energy via vibration damping. On the other hand, particularly compliant materials, such as rubbers and soft polymers, perform well as dampers, but lack in stiffness [1,2]. In this context, biological natural materials such as wood, bone, and seashells, to cite a few examples, represent excellent examples of composite materials possessing both high stiffness and high damping, and thus combine properties that are generally mutually exclusive. This exceptional behaviour derives from an evolutionary optimization process over millions of years, driven towards specific functionalities, where the natural rule of survival of the fittest has led to the continuous improvement of biological structure and organization. For instance, spider silk, bone, enamel, limpet teeth are examples of materials that combine high specific strength and stiffness with outstanding toughness and flaw resistance [3–8]. In these examples, a hierarchical architecture has often been proved to be the responsible for many energy dissipation and crack deflection mechanisms over various size scales, simultaneously contributing to exceptional toughness[2]. Given these numerous examples and the related interesting properties, the rich research field of biomimetics has emerged, with the aim of drawing inspiration from natural structures and implementing them in artificial systems, to bring progress to many technological domains.

Despite rapid progress in the field, studies in biomechanics and biomimetics linking material structure to function have mainly been limited to the quasistatic regime, while the dynamic properties of these materials have been somewhat less investigated, although notable examples of impact tolerance (e.g., the bombardier beetle's explosion chamber [9]) or vibration damping (e.g., the woodpecker skull [10]) have been studied. In fact, the first attempt to analyse biological

vibration isolation mechanisms in the woodpecker date as far back as 1959, when Sielmann[11] found, through dissection and observation, that the cartilage in sutures in its skull have the effect of buffering and absorbing vibration[11]. Furthermore, recent studies have shown that structural hierarchy, which is typical of biological materials, can enhance the performance of artificial metamaterials [12,13]

As confirmed by these examples, it is reasonable to assume that biological structures whose main function is vibration and impact damping, sound filtering and focusing, transmission of vibrations, etc., have also been optimized through evolution, and that it is possible to look for inspiration in Nature for technological applications based on these properties. Based on this assumption, a growing interest in the superior vibration attenuation properties of biological systems has emerged, and nowadays, applications such as bio-inspired dampers are beginning to be used in the protection of precision equipment and the improvement of product comfort[14]. Motivated by this emerging field of research, we provide here a review of some of the main biological systems of interest for their dynamic properties, focusing on the role of structural architecture for the achievement of superior performance.

2. Impact resistant structures

2.1 Mantis shrimp

Probably the most well-known example of impact resistant structure in Nature is the stomatopod dactyl club. The mantis shrimp (*Odontodactylus scyllarus*) is a crustacean with a hammer-like club that can smash prey (mainly shells) with very high velocity impacts [15–17], reaching accelerations of up to 10000 *g*, and even generating cavitation in the water [18]. To sustain repeated impacts without failing, the claw requires extreme stiffness, toughness and

impact damping, and has emerged as one of the main biological systems that epitomizes biological optimization for impact damage tolerance [19].

The exceptional impact tolerance is obtained thanks to the graded multiphase composition and structural organization of three different regions in the claw (Figure 1). The impact region, or striking surface, is dominated by oriented mineral crystals (hydroxyapatite), arranged so that they form pillars perpendicular to the striking surface. A second region called the "periodic region" backs up the impact zone and is mainly constituted by chitosan. This area, which lies just beneath the impact zone, is stacked at different (helicoidal) orientations, generating crack stopping and deviation. Thus, the structure consists of a multiphase composite of oriented stiff (crystalline hydroxyapatite) and soft (amorphous calcium phosphate and carbonate), with a highly expanded helicoidal organization of the fibrillar chitinous organic matrix, leading to effective damping of high-energy loading events [19,20]. The impact surface region of the dactyl club also exhibits a quasi-plastic contact response due to interfacial sliding and rotation of fluorapatite nanorods, leading to localized yielding and enhanced energy damping [21].

Interestingly, it has been found that the mantis shrimp also displays another highly efficient impact damping structure, since it has evolved a specialized shield in its tail segment called a telson, which absorbs the blows from other shrimps during ritualized fighting[22]. The telson is a multiscale structure with a concave macromorphology, ridges on the outside and a well-defined pitch-graded helicoidal fibrous micro-architecture on the inside, which also provides optimized damage tolerance [23,24].

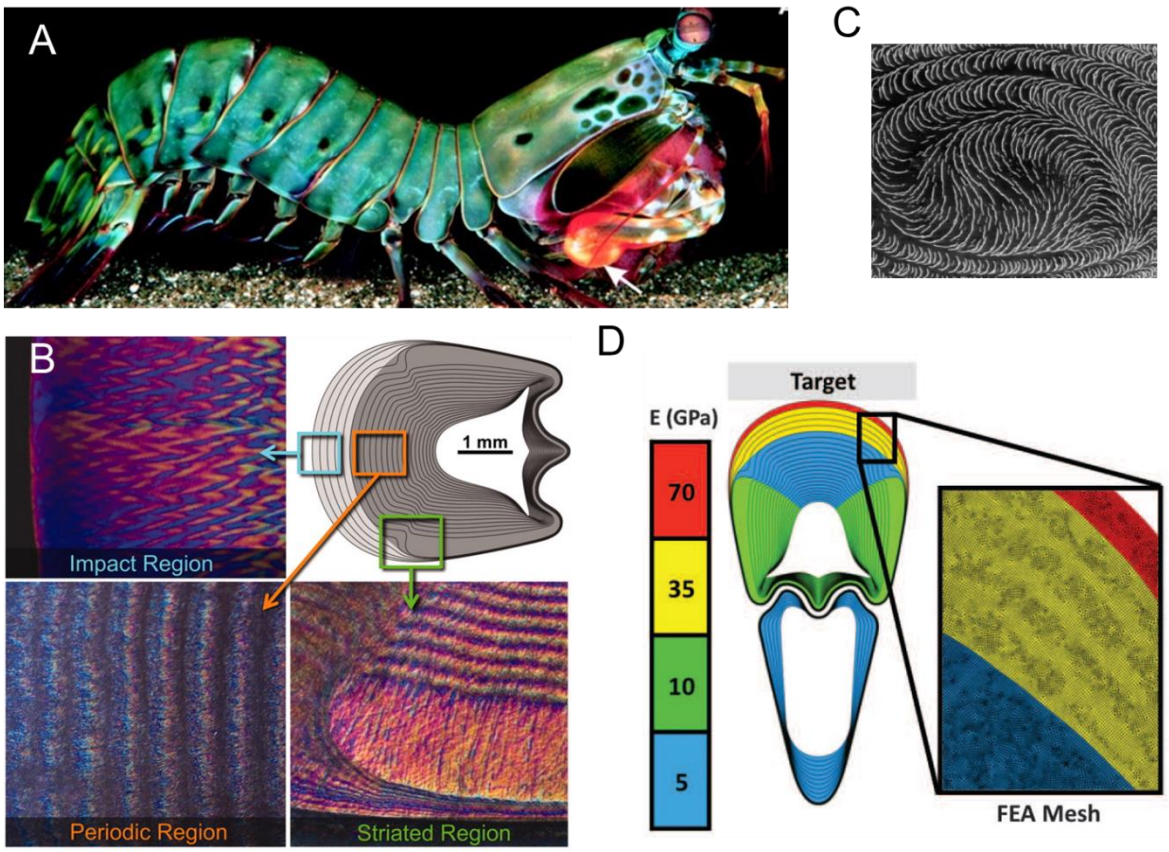

Figure 1: A) Peacock mantis shrimp, with highlighted raptorial dactyl clubs to strike hard objects (adapted from [18]); B) Morphological features of the clubs, in cross-section view, divided in an impact region, a periodic region and a striated region; C) Scanning electron micrograph of the coronal cross-section, showing reinforcing fibre helicoidal arrangement; D) schematic of a Finite Element model accounting for graded material properties (adapted from [19]).

2.2 Woodpecker skull

Another well-known example in Nature of a highly impact-resistant system is that of the woodpecker skull and beak, which repeatedly strikes wooden surfaces in trees at a frequency of about 20 Hz, a speed of up to 7 m/s, and can reach accelerations of the order of 1200 *g*, while avoiding brain injury [10,25]. This structure has been widely studied to draw inspiration for

impact-attenuation and shock-absorbing applications and biomimetic isolation [14]. Limiting our observations to the head, and neglecting the body, feathers, and feet (which could also play a role), the woodpecker emerges as a very complex and rich system, from the mechanical and structural point of view at different spatial scales: macro-, micro- and nanoscale. The head is mainly formed by the beak, hyoid bone, skull, muscles, ligaments, and brain [26].

Several groups have investigated the mechanical behaviour of the woodpecker using finite element analysis [26–32]. Generally, the models are based on the images obtained by X-ray computed tomography (CT) scans. The stress distribution due to the impacts due to pecking is investigated. In some of these studies, the results are also compared with *in vivo* experiments, where the pecking force is measured by using force sensors and compared with that in other birds [27]. Zhu et al. [31] measured the Young's modulus of the skull, finding a periodic spatial variation, as reported in Figure 2A. Moreover, they performed a modal analysis on the skull by using a finite element model (Figure 2B), based on CT scan images, and determining the first ten natural frequencies, as shown in Figure 2C. The largest amplitude frequency components appear at 100 Hz and 8 kHz, which are well separated from the working frequency (around 20 Hz) and the natural frequencies (as derived in simulations), thus ensuring protection of the brain from injury.

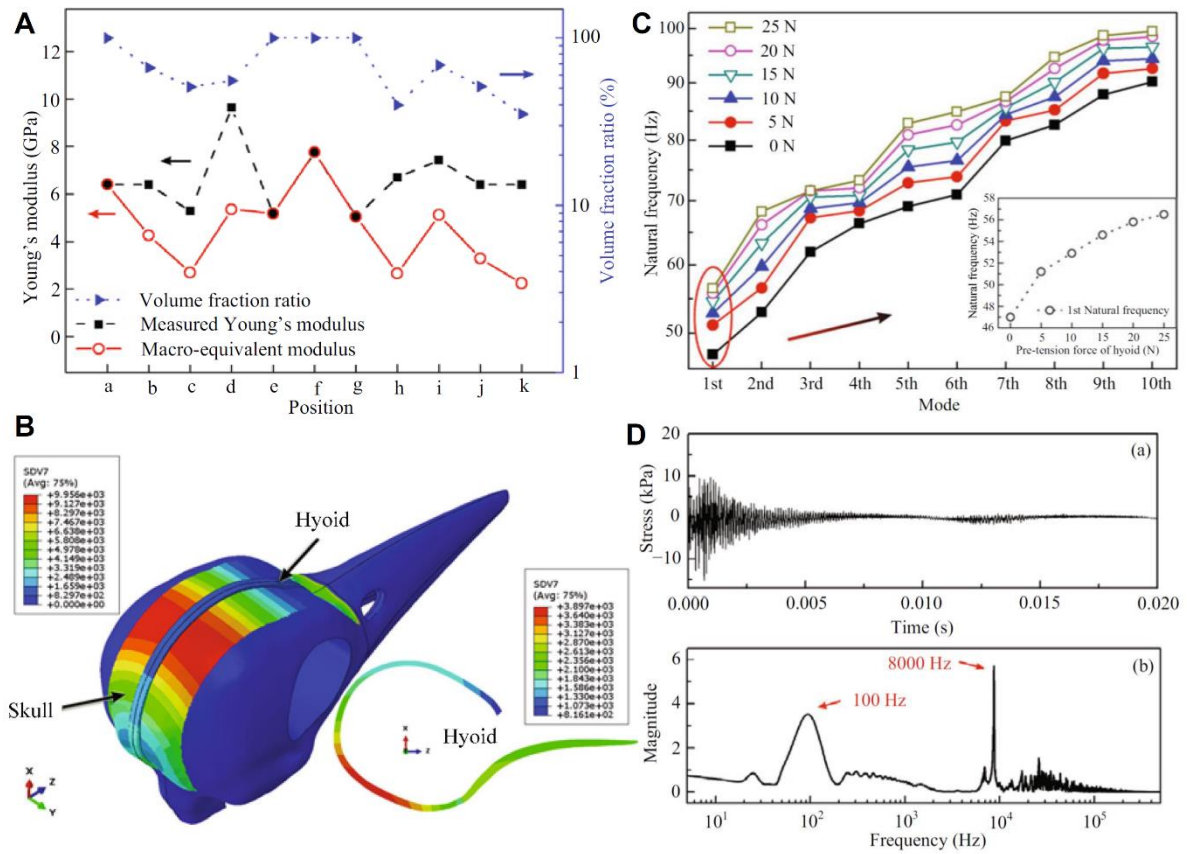

Figure 2 : Vibration attenuation in the woodpecker skull (adapted from [31]). A): Volume fraction ratio of skull bone, local measured modulus, and macro-equivalent modulus around the skull. B): 3D finite-element model of the skull and hyoid bone, with spatial variation of the Young's modulus in the skull. C): first ten modes of the skull under a pre-tension on the hyoid in the range 0-25 N. D), upper panel: stress wave at a brain location under impact direction; lower panel: stress spectrum in the frequency domain obtained by FFT.

Although the results from different groups are not always in agreement, most researchers conclude that the shape of the skull, its microstructure and material composition are all relevant for the exceptional impact-attenuation properties in woodpeckers [10]. In particular, a grading in the bone porosity and mechanical properties is particularly important in damping high frequency vibrations, which can be particularly harmful [33]. Many papers also point out the

importance of the hyoid bone, very peculiar in woodpeckers, in the shock-absorption capability[34]. The hyoid is much longer than in other birds and wraps the skull until the eye sockets, forming a sort of safety belt around the skull. A specific study of the hyoid bone has been carried out by Jung et al. [34], who performed a macro- and micro-structural analysis of the hyoid apparatus and hyoid bones. The authors developed a 3D model of the hyoid which they showed it to be formed by four main parts connected by three joints. Interestingly, by performing nanoindentation measurements, they also showed that it features a stiffer, internal region surrounded by a softer, porous outer region which could play an important role in dissipating the energy during pecking. Another important issue is the relative contribution of the upper and lower beaks in the stress wave attenuation [27,35] which is most probably dissipated through the body [32].

Yoon and Park [10] showed that simple allometric scaling is not sufficient to explain the shock-absorbing properties of the woodpecker. Furthermore, they investigated its behaviour by using a lumped element model including masses, springs, and dampers, as shown in Figure 3A. Given the difficulty in modelling the complexity of the sponge-like bone within the skull with lumped elements, the authors characterized its behaviour by using an empirical method consisting of close-packed SiO_2 microglasses of different diameter (Figure 3B). The vibration transmissibility shows that the porous structure absorbs excitations with a higher frequency than a cut-off frequency which is determined by the diameter of the glass microspheres, as reported in Figure 3C.

Lee et al. [33] reported a detailed analysis on the mechanical properties of the beak, showing that the keratin scales are more elongated than in other birds and the waviness of the sutures between them is also higher than for other birds (1 for woodpecker, 0.3 for chicken and 0.05 for toucan), most probably to favour energy dissipation due to the impact. Raut et al. [36] designed flexural waveguides with a sinusoidal depth variation inspired by the suture geometry of the

woodpecker beak which were tested by finite element analysis. The suture geometry helps reducing the group speeds of the elastic wave propagation whereas the presence of a viscoelastic material, as is the case for collagen in the beak sutures, significantly attenuates the wave amplitudes, suggesting a promising structure for applications in impact mitigation. Garland et al. [37] took inspiration from the same mechanism of the sliding keratin scales in the beak to design friction metamaterials for energy adsorption.

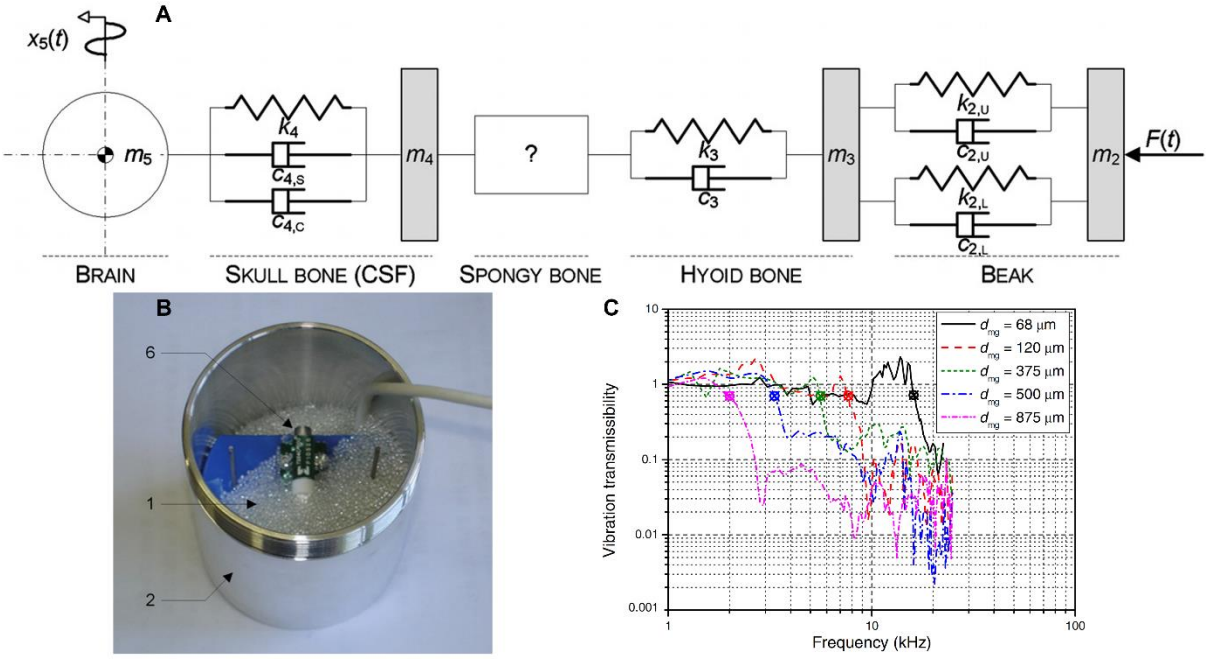

Figure 3 : Modelling of vibration attenuation in the woodpecker skull (adapted from [10]). A): lumped-elements model of the head of a woodpecker. B): empirical model of the spongy bone by means of an aluminium enclosure filled with glass microspheres. C): vibration transmissibility as a function of frequency for different diameters of the SiO2 microspheres.

2.3 Seashells

Seashells are rigid biological structures that are considered to be ideally designed for mechanical protection, and they are now viewed as a source of inspiration in biomimetics [38,39].

A seashell is essentially a hard ceramic layer that covers the delicate tissues of molluscs. Many gastropod and bivalve shells have two layers: a calcite outer layer and an iridescent nacre inner layer. Calcite is a prismatic ceramic material composed of strong yet brittle calcium carbonate ($CaCO_3$). Nacre, on the other hand, is a tough and pliable substance that deforms significantly before collapsing [40]. It is considered that a protective structure that combines a hard layer on the surface with a tougher, more ductile layer on the interior optimizes the impact damping properties [39–41]. When a seashell is exposed to a concentrated stress, such as a predator's bite, the hard ceramic covering resists penetration while the interior layer absorbs mechanical deformation energy. Overloading can cause the brittle calcite layer to fracture, causing cracks to spread into the soft tissue of the mollusc. Experiments have demonstrated that the thick nacreous layer can slow and eventually halt such fractures, delaying ultimate shell collapse. Although a significant amount of research has been performed on the structure and characteristics of nacre and calcite, there has been little research done on how these two materials interact in real shells. While there is evidence that nacre is tuned for toughness and energy absorption, little is known about how the shell structure fully utilizes its basic constituents, calcite, and nacre.

One method employed to analyse the geometry of the shell at the macroscale, while accounting for the micromechanics of the nacreous layer, is to adopt multiscale modelling and optimization [39]. Different failure modes are possible depending on the geometry of the shell. On the other hand, according to optimization procedures, when two failure modes in different layers coincide, the shell performs best in avoiding sharp penetration. To reduce stress concentrations, the shell construction fully leverages the material's capabilities and distributes stress over two different zones. Furthermore, instead of converging to a single point, all parameters converge to a restricted range inside the design space.

According to the experiments done on the two red abalone shells [39,42] the actual seashell arranges its microstructure design to fully utilize its materials and delay failure, a result that is also obtained through optimization. The crack propagates over the thickness of the shell in three different failure situations. Furthermore, the seashell, which is constructed of standard ceramic material, can resist up to 1900 N when loaded with a sharp indenter, which is an impressive load level given its size and structure.

2.4 Suture joints

Suture joints with different geometries are commonly found in biology from micro to macro length scales (Figure 4A) [43]. Examples include the carapace of the turtle [44,45], the woodpecker beak [33], the armoured carapace of the box fish [8,46], the cranium [47], the seedcoat of the *Portulaca oleracea* [48] and *Panicum miliaceum* [49], the diatom *Ellerbeckia arenaria* [50] and the ammonite fossil shells [51], among others.

In the aforementioned systems, the suture joint architecture, where different interdigitating stiff components, i.e., the teeth, are joined by a thin compliant seam, i.e., the interface layer, allows a high level of flexibility and is the key factor for the accomplishment of biological vital functions such as respiration, growth, locomotion and predatory protection [52–54]. Also, from a mechanical point of view, it has been demonstrated computationally and/or experimentally that this particular configuration allows an excellent balance of stiffness, strength, toughness, energy dissipation and a more efficient way to bear and transmit loads [54–58].

Several existing studies confirm this aspect. Among others [53,59], where, in the case of cranial sutures, it emerges that an increased level of interdigitation, found among different mammalian species, leads to an increase in the suture's bending strength and energy storage. Emblematic is the case of the leatherback sea turtle (Figure 4B), a unique specie of sea turtle having the capacity to dive to a depth of 1200 m [60]. This is due to the particular design of the turtle's

carapace, where an assemblage of bony plates interconnected with collagen fibres in a suture-like arrangement is covered by a soft and stretchable skin. As reported in [60], the combination of these two elements provides a significant amount of flexibility under high hydrostatic pressure as well as exceptional mechanical functionality in terms of stiffness, strength and toughness, the collagenous interfaces being an efficient crack arrester. In addition, the study in [61] explained not only how the high sinuosity and complexity of the suture lines in ammonites (Figure 4C) are the result of an evolutionary response to the hydrostatic pressure, but also that the stress, displacements and deformations significantly decrease with the level of complexity. A similar result is also obtained in [62], which seeks to clarify the functional significance of the complex suture pattern in ammonites.

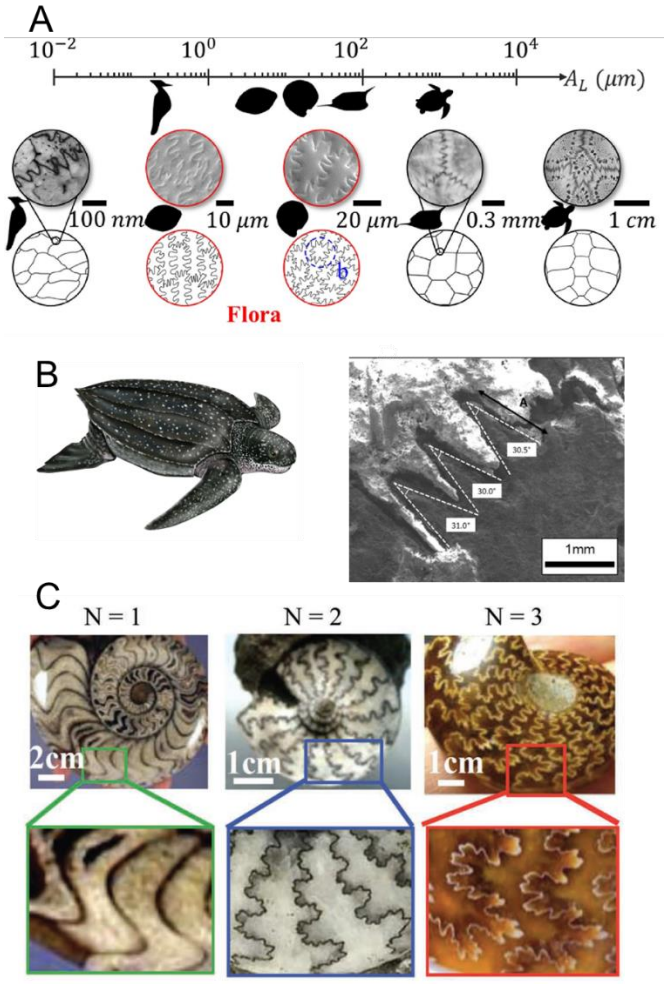

Figure 4: Biological systems with suture tessellation: A) examples from Flora and Fauna (adapted from [58]); B) the leatherback turtle shell (adapted from [60]); C) Hierarchical sutures of increasing complexity found in ammonites (adapted from [63]).

2.5 Bone

Bone has an extremely complex structure, encompassing seven levels of hierarchical organization, from nanocomposite mineralized collagen fibril upwards [64]. Based on this building block, varying mineral contents and microstructure allow to construct various types of tissue for different functionalities, e.g. withstanding tension, resisting impacts, supporting bending and compression. Human cortical bone consists of cylindrical Haversian canals, each surrounded by multilayers of bone lamellae ~10 μm thick, which have a rotated plywood structure in which mineralized collagen fibrils (~100 nm in diameter) rotate from the transverse direction to the longitudinal direction across five sublayers. The fibrils are cemented together by extrafibrillar minerals and noncollagenous proteins [6]. Hierarchical structure plays a fundamental role in bone's exceptional mechanical properties. Bone's trabecular structure and hierarchy is responsible for its unmatched tensile strength, anisotropy, self-healing and lightweight properties [64,65], but also dynamic properties like impact damping [66,67]. Bio-inspiration from bone structures has been exploited to seek enhanced static properties, strength and toughness [68], but relatively limited works have investigated it for dynamic applications. Ultrasonic wave measurements in bone to measure propagating velocity and attenuation have been performed for many years in various settings [69], including "wet" bone [70], showing that hydration is fundamental in defining dynamic properties. Studies in ultrasonics have typically focused on non-destructive evaluation of the bone structure [71,72]. It has also been shown that modal damping can be useful to detect bone integrity and osteoporosis [73], also supported by ultrasonic wave propagation simulations in cancellous bone [74]. Dynamic measurement methods

assessing modal damping have also been used to validate bone models [75]. In terms of bioinspiration, the porous structure of trabecular (rod or truss-like structure) or velar bone (sail-like structure) is of particular interest, due to its lightweight and impact damping characteristics. Most of the work on such 3D frame structures [76] has addressed static properties [77]. However, recent articles have also addressed wave propagation [78,79] and impact loading [80]. Frame structures offer a convenient way to approximate trabecula using truss-like structures, inspired by the well-known Bravais lattices [81]. The implementation of such lattices could pave the way to a simplified model of the bone structure, where the joints can be collapsed to point-like connections and the number of degrees of freedom can be drastically reduced.

2.6 Attenuation of surface gravity waves by aquatic plants

If one considers damping of low frequency vibrations over long timescales, one can look to natural barriers that allow to prevent or delay coastal erosion, and the destruction of the corresponding habitats. One such example is the *Posidonia Oceanica*, a flowering aquatic plant endemic of the Mediterranean Sea, which aggregates in large meadows forming a Mediterranean habitat. This macrophyte has evolved by angiosperms typical of the intertidal zone and displays features similar to that of terrestrial plants: it has roots and very flexible thin leaves of about 1 mm thickness and 1 cm width, without significant shape variations along the leaf length. The anchoring to sandy bottoms is provided by the horizontal growth of the rhizomes, which also grow in vertical. The leave length varies throughout a year due to the seasonal cycle and the marine climatic conditions and can vary as much as 0.3 m in winter and 1 m in summer.

The effects of seagrasses on unidirectional flows are well studied at different scales in the field and in laboratory flumes and in numerical studies, while much less is known about the interaction between seagrass and waves. Wave attenuation due to *Posidonia* and flow

conditions over and within vegetation fields have been investigated experimentally [82] and numerically [83]. It was found that the *Posidonia* is a good natural candidate for dissipating surface gravity waves in coastal regions. The study assessed quantitatively the physical value of the seagrass ecosystem restoration in this area, also opening new routes of action towards a resilient, efficient, and sustainable solution to coastal erosion. Other natural barriers to water wave propagation, other than vegetation such as the *Posidonia*, exist and are fundamental. For example, ice covering the surface of the ocean around Antarctica and the Artic Sea represents an important wave attenuation medium for slowing down the disintegration of the polar ice shelves. Quantitative measurements of such attenuation have been recently obtained through stereoscopic measurements [84].

2.7 Attenuation of surface seismic waves by trees

Further recent evidence of natural barriers for large scale vibrations is the attenuation of seismic surface waves achieved by trees [85]. The vibrations are transmitted to the trees through two coupling mechanisms, associated with two distinct vibrational modes. At high frequency (around 50 Hz), the longitudinal motion of the trees perpendicular to the soil surface is responsible for a high scattering effect on the surface wave and a hybridization to bulk shear waves. This means that the soil surface is mechanically blocked by the trees around those frequencies. In the low frequency range, below 1 Hz, the flexural motion of the trees induces different coupling effects on surface wave propagation. The flexural motion creates a bending moment at the soil/tree interface with can create long range coupling phenomena. Flexural resonances for the trees generally fall in the same frequency band as the micro-seismic noise produced by the ocean (between 0.3 and 0.8 Hz, detectable all over the world), which suggest a potential use of these frequencies to monitor the growth process of the trees and the evolution of their surrounding environment [86].

2.8 Conclusions on impact resistant structures

From the examples seen in the previous Sections, it emerges that impact-resistant biological structures have a number of common features. The first is related to a complex hierarchical architecture spanning from the nano- to the macro-scale, as in the case of the woodpecker skull or suture joints. Hierarchy, in particular, allows the system to be multifunctional and to accomplish both biological and mechanical functions in an optimized fashion. Additionally, in terms of dynamical behaviour, hierarchical structure allows to simultaneously address various size scales and therefore frequency ranges. The second characteristic is heterogeneity, enabling natural materials to combine the desirable properties of their building blocks, which are typically light, widely occurring materials: polymeric and ceramic for mineralized systems or crystalline and amorphous phases for non-mineralized ones. Heterogeneity allows Nature to create hierarchical composites that perform significantly better than the sum of their parts. Typically, the stiffer phase provides rigidity and strength while the soft phase increases ductility. This distinctive quality leads, for example, to the exceptional impact damping properties of the seashells described above. Another common trait of impact-resistant biological structures is porosity, which plays an important role in dissipating impact energy and, at the same time, allows to decrease the overall weight of the system. Finally, the occurrence of complex geometrical features is a characteristic commonly found in impact-resistant structures in biology. The high sinuosity of the suture lines in ammonites or the helicoidal organization of the mantis shrimp's dactyl clubs are examples of this, and direct evidence of their continually optimized nature, deriving from adaptation to the form that best achieves the required function.

3. Sensing and predation

3.1 Spider webs

Of all the natural structures that inspire and fascinate humankind, spider orb webs play a particularly central role and have been a source of interest and inspiration since ancient times. Spiders are able to make an extraordinary use of different types of silks to build webs which are the result of evolutionary adaptation and can deliver a compromise between many distinct requirements [87], such as enabling trapping and localizing prey, detecting the presence of potential predators, and serving as channels for intraspecific communication [88]. The variety of structures, compositions, and functions has led to the development of a large amount of literature on spider silks and webs [88–90] and their possible bio-inspired artificial counterparts [91,92].

The overall mechanical properties of spider orb webs emerge from the interaction between at least five types of silk [3,93], each with a distinct function in the web. The most important vibration-transmitting elements are made from the strong radial silk [94], which also absorbs the kinetic energy of prey [95,96] while sticky spiral threads, covered with glue, are used to provide adhesion to retain the prey [97,98]. Moreover, junctions within the webs can be composed of two different types of silk [93]: the strong and stiff piriform silk that provides strength to the anchorages [99,100] (Figure 5A-B), and the aggregate silk that minimizes damage after impacts [5,93] (Figure 5C). The mechanical synergy of such systems is therefore due to the mechanical response of the junctions [101], the constitutive laws of different types of silks, and the geometry of the webs [5]. The richness of these features, which are still the subject of many studies, have already inspired technologies with different goals in various scientific fields [102–104].

Spider orb webs are able to stop prey while minimizing the damage after impacts, thus maintaining their functionality [5], partially exploiting the coupling with aerodynamic damping

that follows prey impacts [96]. This makes orb webs efficient structures for capturing fast-moving prey [105], whose location can then be detected due to the vibrational properties of the orb web. Efficiency in detecting prey by the spider is mediated by the transmission of signals in the webs, which needs to carry sufficient information for the prey to be located [106]. Using laser vibrometry, it has been demonstrated that the radial threads are less prone to attenuating the propagation of the vibrations compared to the spirals [87], due to their stiffer nature [107], allowing them to efficiently transmit the entire frequency range from 1 to 10 kHz.

Spiral threads can undergo several types of motion, including: (i) transverse (perpendicular to both the thread and the plane of the web) (ii) lateral (perpendicular to the thread but in the plane of the web), and (iii) longitudinal (along with the thread axis), thus yielding complex frequency response characteristics [108–110]. Distinct wave speeds are also associated with each type of vibration, i.e., transverse wave speed is determined by string tension and mass density, while longitudinal wave speed is linked to mass density and stiffness [111]. With the addition of more reinforcing threads due to the multiple lifeline addition by the spider, the orb webs appears to maintain signal transmission fidelity [112]. This provides further evidence of the impressive optimization achieved in these natural structures, which balance the trade-offs between structural and sensory functions.

The sonic properties of spider orb webs can also be significantly influenced by pre-stressing, as demonstrated in the study conducted by Mortimer et al. [113]. Wirth and Barth [114] have shown that silk thread pre-stress increases with the mass of the spider, considering both inter and intra-specific variations, and may be used to facilitate the sensing of smaller prey [115]. The pre-tension in webs can also be strongly influenced by large amplitude vibrations, as demonstrated by numerical analysis [116]. This dependence has been shown to be stronger if the structure is damaged, especially in the radial threads [117].

Investigations on the vibration transmission properties of silk have been conducted by accessing its high-rate stress-strain behaviour using ballistic impacts on Bombyx mori silk (which can be partially compared to spider silk) [118]. Some studies indicated that the capability of transmitting vibrations is relatively independent of environmental conditions such as humidity [119,120], but in general it is expected that they affect the silk Young's modulus and the pre-stress level on the fibres, and therefore the speed of sound (i.e., wave propagation speed) in the material [121–123]. This dependence is one of the reasons why the measurement of the speed of sound in silk has not produced homogeneous data [109,124,125], and could provide a possible degree of freedom for spiders in tuning the vibrational properties of their webs [113,124].

Spider orb webs have proven to be one of the most inspiring systems to design structures able to manipulate elastic waves. Although many types of webs can be extremely efficient in detecting and stopping prey [126], plane structures tend to be preferred when it comes to bio-inspired systems, due to their simplicity. Metamaterials can be designed exploiting the rich dynamic response and wave attenuation mechanism of orb webs [127], based on locally resonant mechanisms to achieve band gaps in desired frequency ranges [128], and further optimized to achieve advanced functionalities [129]. The possibility of designing low-frequency sound attenuators is also regarded as a common objective in metamaterials design, and spider web-inspired structures seem to be able to provide lightweight solutions to achieve this goal [130,131].

3.2 Spider sensing

Although many spiders have poor sight, remarkable sensors that make them capable of interacting with their surroundings have evolved [132], including hair-shaped air movement detectors, tactile sensors, and thousands of extremely efficient strain detectors (lyriform organs such as slit sensilla) capable of transducing mechanical loads into nervous signals embedded in their exoskeleton [133–135]. Air flow sensors, named trichobothria (Figure 5D), seem to be

specifically designed to perceive small air fluctuations induced by flying prey, which are detectable at a distance of several centimetres [136]. Spiders can process these signals in milliseconds and jump to catch the prey using only the information about air flow [137]. Although this could be sufficient to guide the detection of the prey using trichobothria, it could be that different hair-like structures undergo viscosity-mediated coupling that affects the perception efficiency. Interestingly, in the range of biologically relevant frequencies (30−300 Hz), viscous coupling of such hair-like structures is very small [138]. It seems, in particular, that the distance at which two structures do not interact is about 20 to 50 hair diameters, which is commonly found in Nature [138,139]. Spiders are also equipped with strain sensors (lyriform organs), which are slits that occur isolated or in groups (Figure 5E) with a remarkable sensory threshold in terms of displacement (from 1.4 nm to 30 nm) and corresponding force stimulus (0.01 mN). Moreover, many of such organs have an exponential stiffening response to stimuli, which makes them suitable to detect a wide range of vibration amplitudes and frequencies. These organs act as filters with a typical high-pass behaviour [140] to screen the environmental noise found in Nature. Despite their remarkable capability in detecting vibration patterns (in frequencies between 0.1 Hz and several kHz), it is not yet clear how low-frequency signals are transmitted [141]. In any case, spider impact sensing on orb webs has been shown to be an intricate mechanism determined by both material properties and web structure [142].

The sensing capabilities of spiders have driven the design of bio-inspired solutions in terms of sensor technology. Materials scientists have designed bio-inspired hair sensors realized to work both in air [143,144] and water [145]. Furthermore, the lyriform organs have inspired crack-based strain sensors [146,147], eventually coupled with the mechanical robustness of spider silk [146]. Interestingly, these two types of structures (crack and hair sensors) may be combined in a multi-functional sensor. Results for such a spider-inspired ultrasensitive flexible vibration sensor demonstrated a sensitivity that outperforms many commercial counterparts [147].

Spider silk threads are also capable of detecting airflows by means of their fluctuation [148], providing an incredibly wide range of detectable frequencies, from 1 Hz to 50 kHz. Thus, by modifying these materials (e.g., making them conductive) it may be possible to produce devices able to expand the range of human hearing. It is clear, however, that many difficulties remain to be resolved to scale and fully optimize such bio-inspired solutions. Firstly, the reduction of the exposed surface can be large due to the need to integrate a sensor in the electronics. Secondly, wearing and application of the device could mechanically deteriorate its efficiency during its lifetime. Lastly, an engineering approach is in stark contrast with biological ones. In this context, a profound breakthrough is needed to achieve high efficiency in the self-assembly materials at the submicron scale.

3.3 Scorpion sensing

Scorpions are arachnids belonging to the *Subphylum Chelicerata* family of the arthropods (which includes spiders), which have evolved sensory mechanisms specially adapted to desertic environments [149]. Once structure-borne vibrations are produced in the ground, they propagate through bulk and surface waves: while the former propagate into the soil at large speeds and cannot be perceived by surface-dwelling animals, the latter can provide a useful information propagation channel for various species [150,151]. Sand offers an especially interesting medium in this regard, since its wave speed and damping are significantly lower than in other soils, favouring time-domain discrimination and processing [152]. Brownell [153] has shown that two types of mechanoreceptors can be observed in the *Paruroctonus Mesaensis* desert scorpion species: (i) sensory hairs on the tarsus, which sense compressional waves, and (ii) mechanoreceptors located at the slit sensilla, which sense surface waves, thus serving as the basis for the scorpion's perception of the target direction, performing a role of mechano-transduction similar to that observed in spiders [154]. Thus, these structures appear to be those responsible for vibration sensing in scorpions, even though some controversy exists regarding

the use of other scorpion appendages for the same purpose [155]. Brownell and Farley have shown that this scorpion species can discriminate the vibration source direction by resolving the time difference in the activation of the slit sensilla mechano-receptors even for time intervals as small as 0.2 ms [156]. The same authors have also shown that for short distances (down to 15 cm), scorpions can discriminate not only direction but also distance and vibration signal intensities, which are means to distinguish between potential prey from potential predators [157]. Such underlying phenomena have been used to construct a computer theory that simulates prey-localizing behaviour in scorpions [158], further motivating the development of artificial mechanisms based on this approach. Microstructural investigations as the ones performed by Wang et al. [159] have demonstrated that the slit sensilla owe their micro-vibration sensing properties to their tessellated crack-shaped slits microstructure [160], further indicating that this type of microstructure can serve as a bioinspiration for the design of new mechano-sensing devices [146,161].

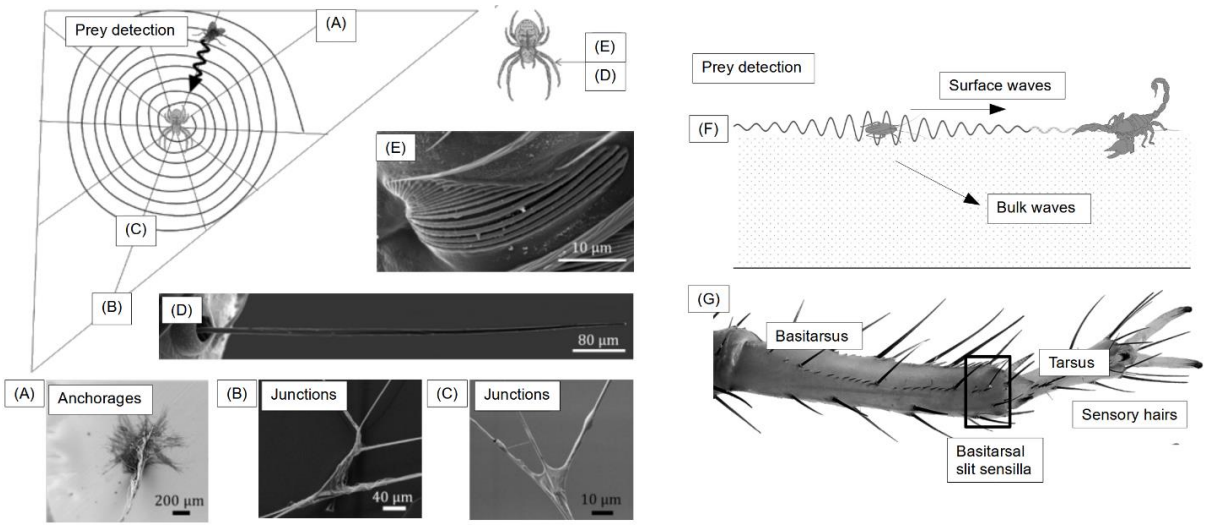

Figure 5: Prey sensing similarities in spiders and scorpions. A) web structure: a typical orb web of a spider Nuctenea umbratica. The web is built by means of junctions between threads and surfaces, B) junctions between radial threads, C) and junctions between radial and spiral threads. A flying prey can be eventually detected by air flow sensors, D) the tricobothria. If the

prey impacts the web, the vibrational signal will be transmitted mainly by radial threads and be perceived by E) lyriform organs of the spider. Figure adapted from [93,132]*. F) schematic of scorpion prey detection using surface waves; G) sensory hairs and mechanoreceptors located at the slit sensilla sense surface waves. Adapted from* [159,162]

3.4 Control of ground-borne sound by mammals

Vibration control in mammals is not restricted to air-borne signals. Many use impacts by "drumming" parts of their bodies to generate vibrations that propagate in the soil. For example, foot-drumming patterns may be found in rabbits or elephant to communicate with other individuals. Unlike in the Cochlea, where the signal is split, and thus analysed, according to its frequency content, foot-drumming is based on the generation and analysis of complex transient vibrational patterns. One of the first species identified to use foot-drumming to communicate is the blind rat [163]. More recent studies have identified the social and environmental monitoring purposes associated with this communication channel in elephants [164–166].

3.5 Anti-predatory structures and strategies

It is thought that the origin of many distinctive morphological and/or behavioural traits of living organisms is related to the selective pressure exerted by predators [167,168]. Generally, various defensive strategies can be adopted by organisms to reduce the probability of being attacked or, if attacked, to increase the chances of survival. The first consists in avoiding detection (i.e., *crypsis*), through camouflage, masquerade, *apostatic* selection, subterranean lifestyle or nocturnality, and deterring predators from attacking (i.e., *aposematism*) by advertising the presence of strong defences or by signalling their unpalatability by means of warning coloration, sounds or odours [169]. The second are based on overpowering, outrunning and

diverting the assailants' strikes by creating sensory illusions to manipulate the predator's perception [170–172].

Despite being extremely fascinating from an engineering point of view, the effectiveness of the first type of defensive strategies is restricted mainly to visual phenomena and none of them work on non-visually oriented predators. However, although rare, several acoustic based deflection strategies exist in Nature. Most of them are related to one of the most famous examples of non-visually oriented predators, i.e., echolocating bats (Figure 6A) that rely on echoes from their sonar cries to determine the position, size and shape of moving objects in order to avoid obstacles and intercept prey in the environment [168,173–175].

The first strategy to avoid detection by bats can be seen in some species of earless moth that, as a result of millions of years of evolution, developed a passive acoustic camouflage relying on a particular configuration of both the thorax and the wings. In particular, differently from the other species of moth which evolved ears to detect the ultrasonic frequencies of approaching bats or produce, when under attack, ultrasound clicks to startle bats and alert them to the moth's toxicity [176–178], the wings of earless moths are covered with an intricate layer of scales (Figure 6B) that serve as acoustic camouflage against bat echolocation [177,179]. According to [177], each leaf-like shaped scale shows a hierarchical design, from the micro-to the nanoscale, consisting, at the larger scale, of two highly perforated laminae made of longitudinal ridges of nanometer size connected by a network of trabeculae pillars. This configuration leads to a highly porous structure which is able, because of the large proportion of interstitial honeycomb-like hollows, to absorb the ultrasound frequencies emitted by bats and thus reduce the amount of sound reflected back as echoes [180]. As a result, the moth partially disappears from the bat's biosonar and the distance at which the bat can detect the moth is reduced by 5-6% [179], representing a significant survival advantage. In addition, by exploring the vibrational behaviour of a wing of a *Brunoa alcinoe* moth, researchers discovered that each scale not only

behaves like a resonant ultra-sound absorber having the first three resonances in the typical echolocation frequency range of bats [177], but also that each one has a different morphology and resonates at a particular frequency, creating a synergistically broadband absorption [180]. As reported in [180], it can be thus said that the complex pattern of scales on moth wings exhibit the key features of a technological acoustic metamaterial.

Another example of an acoustic-based strategy to confuse predators is the long hindwing tail (Figure 6C) commonly found on luna moths (*Actias luna*). Such tail presents a twist toward the end and this distinguishing feature, as suggested in [181], is the key for how the tail creates a sort of acoustic camouflage against echolocating bats. The tail, in particular, because of its length and twisted morphology, in reflecting the bat's sonar calls produces two types of echoic sensory illusions [181]. The first consists in deflecting the bat's attacks from the vital parts of the body, i.e., head and thorax, to this inessential appendage. By using high-speed infrared videography to analyse the bat-moth interactions, according to the authors, in over half of the interactions, bats directed the attack at the moth's tail as the latter created an alternative target distracting from the principal one, i.e., the moth's body. Also, by comparing moths with the tail and moths with the tail ablated, it emerged a survival advantage of about 47%.

The second sensory illusion provided by the twisted tail consists in inducing a misleading echoic target localization that confuses the hunting bats [170,181]. As reported in [181], the origin of this effect is the twist located at the end of the tail that creates a sequence of surfaces having different orientations so that, independently of the inclination of both the incident sound waves and the fluttering moth, the tail is able to return an echo, complicating and spatially spreading the overall echoic response of the moth. In addition, the analysis of the overall acoustic return generated by the wings, body and tail of a Luna moth, revealed an additional survival contribution of the twisted tail, consisting in a shift of the echoic target centre, i.e., the centre

of the echo profile used by the bat to estimate the prey location, away from the moth's thorax [181].

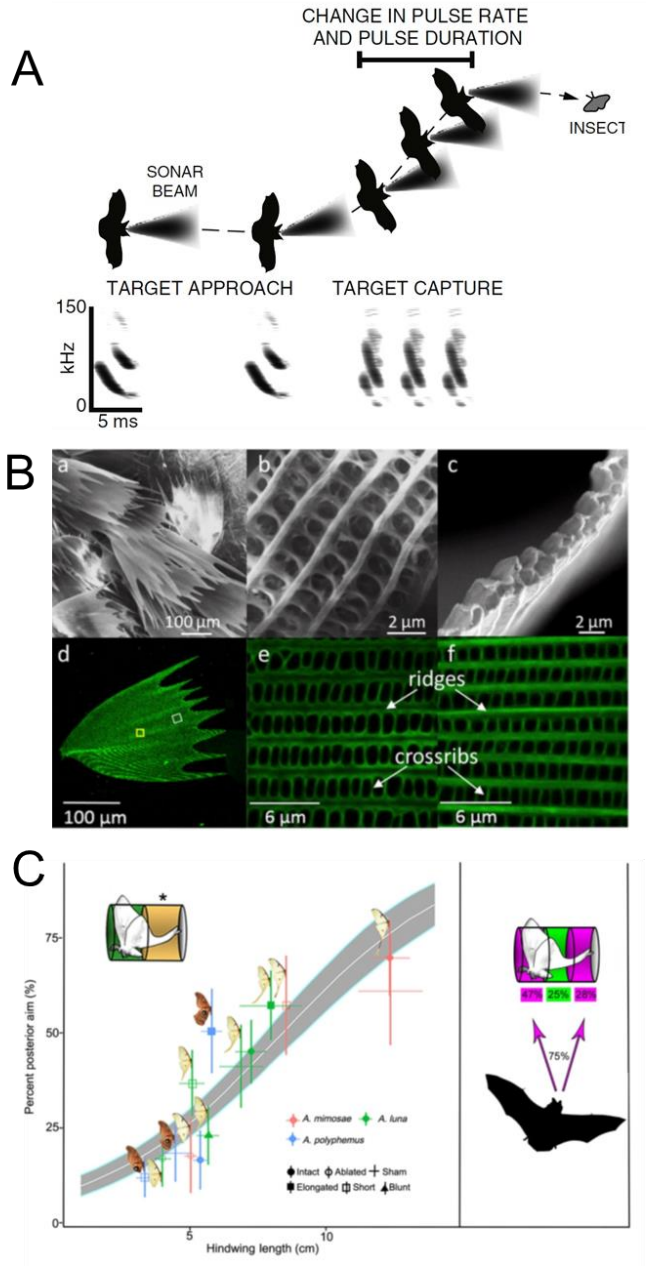

Figure 6: Anti-predatory strategies. A) The high-resolution 3D acoustic imaging system evolved by the echolocating bats (adapted from [182]) and the moth's strategies to avoid being detected: B) appropriate scale arrangement and structure (adapted from[176]). and C) hindwing tails. Behavioural analyses reveal that (A) bats aim an increasing proportion of their attacks at the posterior half of the moth (indicated by yellow cylinder with asterisk) and that (B) bats attacked the first and third sections

572 *of tailed moths 75% of the time, providing support for the multiple-target illusion. An enlarged echo*
573 *illusion would likely lead bats to target the hindwing just behind the abdomen of the moth, at the*
574 *perceived echo centre (highlighted in green); however, bats targeted this region only 25% of the time*
575 *(adapted from* [170]*).*
576
577 As previously mentioned, the second type of passive acoustic camouflage developed by earless
578 moths consists in having much of the thorax covered by hair-like scales (Figure 7A) acting as
579 a stealth coating against bat biosonar[183–185]. As suggested by[185,186] such thoracic scales create
580 a dense layer of elongated piliform elements, resembling the lightweight fibrous materials used
581 in engineering as sound insulators. Their potential as ultrasound absorbers was explored in [185]
582 by means of tomographic echo images and an average of 67% absorption of the impinging
583 ultrasound energy emerged. Also, to provide a more in-depth investigation, the authors
584 employed acoustic tomography to quantify the echo strength of diurnal butterflies that are,
585 contrary to moths, not a target for bat predation. The results were then used to establish a
586 comparison with those derived for moths (Figure 7B). Interestingly, the analysis revealed that
587 the absorptive performance is highly influenced by the scale thickness and density, with the
588 very thin and less dense scales typical of butterflies that can absorb just a maximum of 20% of
589 the impinging sound energy. Conversely, the denser and thicker moth's thorax scales possess
590 ideal thickness values that allow the absorption of large amounts of bat ultrasonic calls. These
591 findings are confirmed by [183] where an extended list of references is also provided.
592

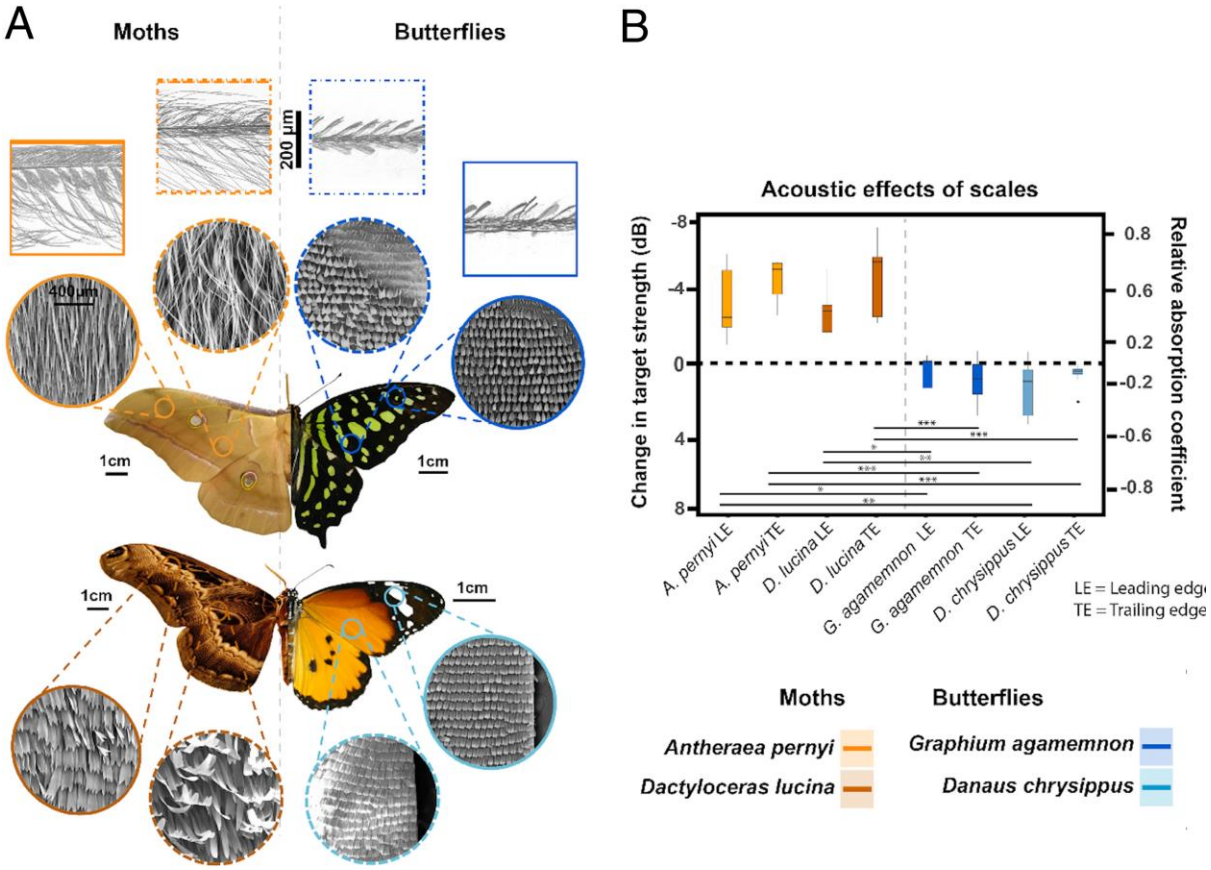

Figure 7: Tiling patterns and acoustic effects of lepidopteran scales: A) SEM images of butterflies Graphium agamemnon and Danaus chrysippus and moths Dactyloceras lucina and Antheraea pernyi, B) Change in target strength caused by presence of scales, and equivalent intensity absorption coefficient (Adapted from[179]).

Finally, airborne sound and vibration signals play an important role in bee communication and defence mechanisms [187]. The thorax of the bee contains a powerful musculature that is used to fly but also to produce vibratory impulses. For a long time, communication between bees seemed to be almost exclusively regulated by chemical signals, i.e. pheromones. In recent decades, it has become increasingly clear that bees live and interact in a world of sound and vibration [187,188]. One particular species, the Japanese bee *Vespa mandarinia japonica*, uses sounds to coordinate and attack predators *en masse*. In particular, the defence mechanism developed by *Vespa mandarinia* relies on the control of dorso-ventral and longitudinal muscles

that do not contract alternately, as in flight, but tense simultaneously while the bee remains motionless. After a few minutes, the temperature of its thorax increases and can reach 43° (maximum temperature). If a foraging hornet tries to enter the hive, more than 500 workers quickly engulf it in a ball to rapidly raise the temperature to 47°C, which is lethal for the hornet but not to the bees [188]. This behaviour is also associated with high neural activity, underlying the bees' computation for the use and production of sounds and vibrations [189].

3.6 Conclusions on structures for sensing and predation

We have seen that structures that perform sensory functions are generally related with localization, allowing a certain species to either perceive its surroundings, localize prey, or escape from predators. Some common and recurring features can be found. In all cases, the sensory capability of an organism benefits from specialized transducers used to detect vibrations (e.g., cuticles for insects and arachnids, silk for spiders). Interestingly, these transducers are often associated with nonlinear constitutive behaviour, e.g., both cuticle [190] and silk [191] present a high stiffening behaviour with an exponential constitutive law. Moreover, this relationship is strongly mediated by water content, which influences the properties of both the cuticle [140,192] and silk [193]. Thus, natural structures often present a strong relationship with a fluid or viscous medium, as an agent capable to confer specific mechanical properties. Generally speaking, the sensing capability is also strongly mediated by the interaction with the substrate (e.g., trees, and leaves for spiders; sand and rocks for scorpions). Another common feature is that the interaction with the environment is also often mediated by air flows sensors, with a common hair-like shape that is present in spiders [136], scorpions [194], crickets [195], and fish [196].

4. Sound/vibration control, focusing and amplification

4.1 Echolocation in Odontocetes

631 Apart from communication purposes, toothed whales and dolphins (Odontocetes) use clicks,
632 sounds and ultrasounds for sensing the surrounding environment, navigating, and locating prey
633 [197]. This process is similar to that adopted by terrestrial animals like bats and is called
634 echolocation [198–200]. The sounds are generated in special air cavities or sinuses in the head, can
635 be emitted in a directional manner [201,202], and their reflections from objects are received through
636 the lower jaw and directed to the middle ear of the animal (Figure 8)[203,204]. A number of studies
637 have adopted CT scans and FEM to simulate sound generation and propagation in the head of
638 dolphins or whales, demonstrating how convergent sound beams can be generated and used to
639 direct sound energy in a controlled manner, and also how sound reception can be directed
640 through the lower jaw to the hearing organs [205,206]. Dible et al. have even suggested that the
641 teeth in the lower jaw can act as a periodic array of scattering elements generating angular
642 dependent band gaps that can enhance the directional performance of the sensing process [207].
643 The emitted frequencies of the sounds used for echolocation are typically in the kHz range,
644 e.g., bottlenose dolphins can produce directional, broadband clicks lasting less than a
645 millisecond, centred between 40 to 130 kHz. Some studies have suggested that high intensity
646 focussed sounds can even be used to disorient prey, although this remains to be confirmed
647 [208,209]. The process of echolocation is extremely sensitive [210,211] and can provide odontocetes
648 with a "3D view" of their surrounding environment world. This is confirmed by the fact that
649 sonar signals employed by military vessels can confuse and distress whales and dolphins, and
650 even lead to mass strandings [212]. Reinwald and coworkers [213] envisaged that the capability,
651 which is still poorly-understood, of dolphins to accurately locate targets over the whole solid
652 angle might be due to the correspondence between the reverberated coda of the signal
653 transmitted along the bone to the ear and the location of the target that generated the signal.

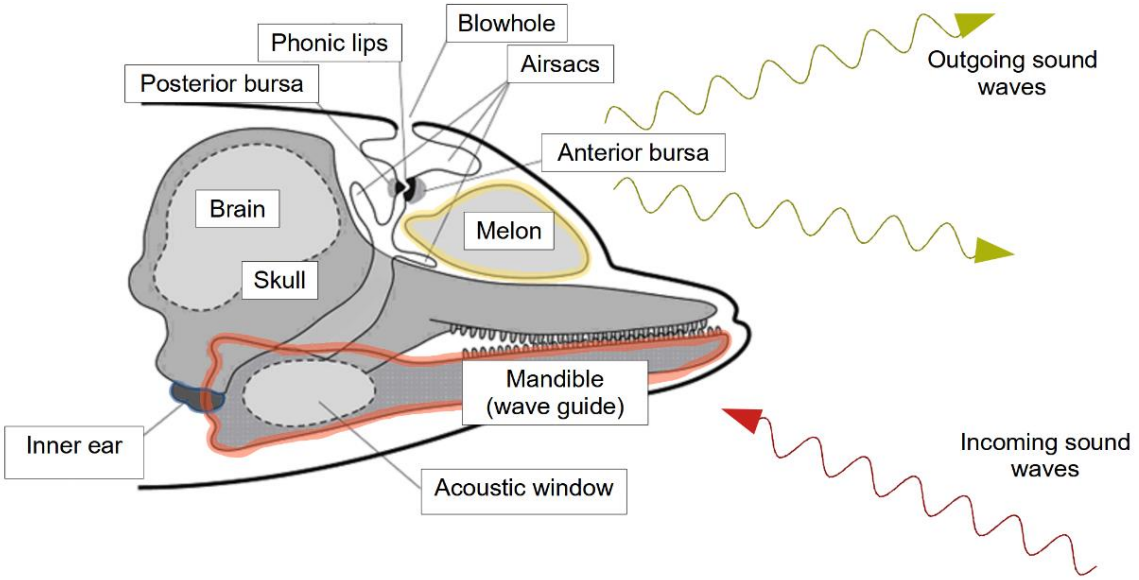

654

655 *Figure 8: Structures for sound production and detection in Dolphins. Modified and adapted*
656 *from*[214].

657

658 **4.2 High amplitude sound generation in mammals**

659 An interesting mechanism exploited in Nature to produce sounds is to develop specific
660 resonating structures attached to the sound-producing organs of animals with the role to
661 selectively filter out some frequencies and amplify others [215]. There are several examples of
662 anatomical adaptations to increase sound radiation efficiency, such as air sacs in frogs [216], birds
663 [217], and mammals (Riede et al., 2008), or enlarged larynges in howler monkeys [218] and
664 hammerhead bats [219]. Some animals even change their environment by constructing horns or
665 baffles that aid in radiating the sound [220]. The case of howler monkeys (*Alouatta*) is particularly
666 interesting: these are widely considered to be the loudest land animals, since their vocalizations
667 can be heard clearly at a distance of 4.8 km. They emit sound at a sound level of 88dB, which
668 means 11 dB per kg - almost 10.000 times louder per unit mass compared to other animals
669 (Figure 9A). The function of howling is thought to relate to intergroup spacing, territory
670 protection and social behaviour, as well as possibly mate-guarding[221]. The extraordinary

capability of these monkeys to produce low frequencies and loud vocalizations has been largely studied and the exact mechanism exploited is still debated [222]. However, two main elements are considered essential in this mechanism: expansion of the hyoid bone into a large shell-like organ in the throat and large hollow air sacs located on either side of the bone (Figure 9B). When the glottis produces low frequency sounds, the hyoid and air sacs function as resonators and the constrictions in the post-glottal structures (a narrow and curved supraglottal vocal tract) reduce the velocity of the air flow, elevating its pressure and, consequently, raising its volume [223]. The harshness of the roars is a result of the forced passage of air, resulting in irregular noisy vibrations. The acoustic function of the air sacs, however, is unclear and not all authors agree on their function as resonators, proposing as an alternative an impedance matching purpose [224] or potentially to suppress resonances [225].

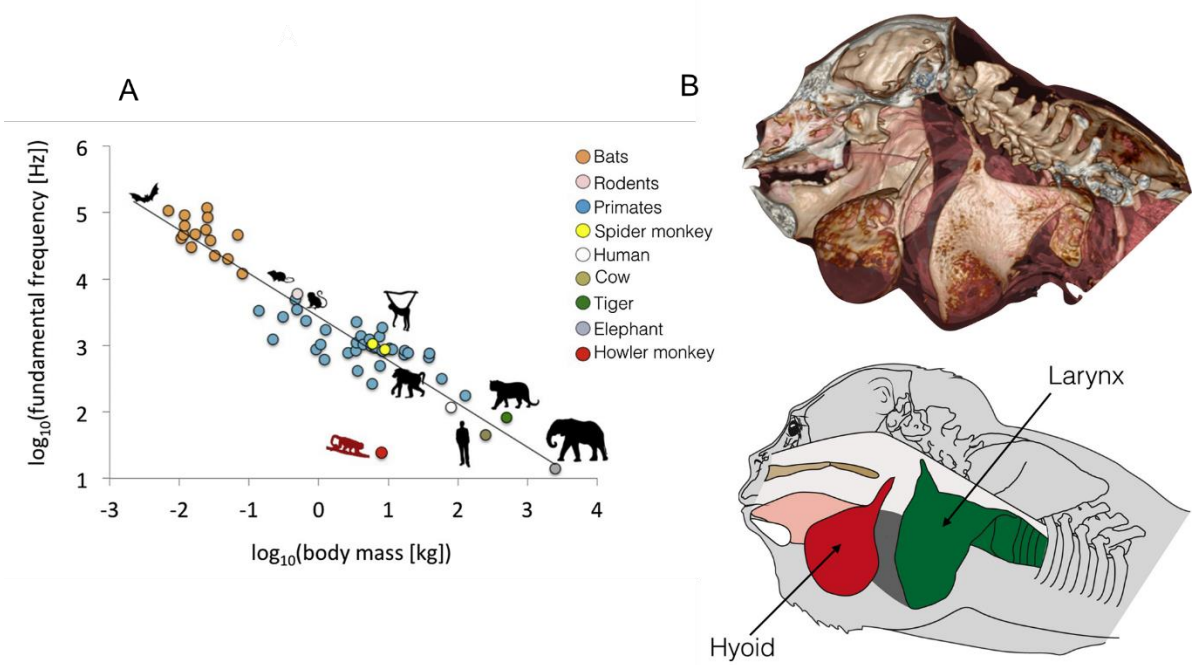

Figure 9: A) The exceptionally low frequency of Howler Monkey vocalizations; B) Howler Monkey vocal apparatus. Adapted from [218].

4.3 Cochlea in mammals

The hearing organ in mammals has developed extraordinary capabilities from the point of view of the extension of audible frequencies and perceived intensities. The human ear (Figure 10A-C), for example, is sensitive to 8 octaves of frequencies (20Hz-20kHz) and is capable of distinguishing sounds within 12 orders of magnitude of intensity (120 dB). The evolutionary complexity of this organ has represented an obstacle to the deep understanding of all the mechanisms involved and, even today, some aspects remain unexplained (for a review on the mechanical mechanisms involved see [226,227]). The *cochlea* (Figure 10E) is the core organ of the inner ear (in blue in Figure 10A), coiled in the form of a snail (hence its name) and enclosed by a bony shell. The cochlea is composed of two ducts (scala vestibuli (SV) and *scala tympani* (ST), see Figure 10B) filled with a liquid (perilymph) which is compressed by a membrane, hit by three miniscule bones of the middle ear (in red in Figure 10A). The pressure difference between the two ducts put in vibration the basilar membrane, which separates them, and which conducts a largely independent traveling wave for each frequency component of the input (this mechanism was proposed for the first time in [228] and then largely developed). Because the basilar membrane is graded in mass and stiffness along its length [229], however, each traveling wave grows in magnitude and decreases in wavelength until it peaks at a specific frequency-dependent position (see Figure 10F), thus allowing a spatial coding of the frequency contents. This is referred to as the tonotopic organization of the cochlea [230]. The mechanical vibration of the basilar membrane is then collected and translated into an electrical impulse from the hair cells (see Figure 10D) and sent to the brain for the signal decoding.

One of the most relevant and studied characteristics of the basilar membrane is that its response to an external stimulus is highly nonlinear (i.e., not proportional to the input amplitude) and this nonlinear response is also frequency specific. Moreover, each point of the cochlea has a different nonlinear response depending on the characteristic frequency pertaining to this

specific point [231,232]. These features are especially evident in *in vivo* measurements, also underling the existence of an active mechanism (otoacoustic emission) added to the merely mechanical ones (see e.g., [233–235]).

The mechanisms at play are complex and often more than a possible explanation can be found in literature, but different simplified models have tried to capture the basic features of the cochlea and reproduce its incredible capacity of sensing, its tonotopic and amplification behaviours (for a review see e.g., [236,237]). One of the aspects that can be relevant for bioinspired applications in the propagation of elastic waves in solids, is the influence of the geometry (spiral) on the frequency attenuation/loss and on the tonotopic property of the sample, as also pointed out by some works (see [238,239]).

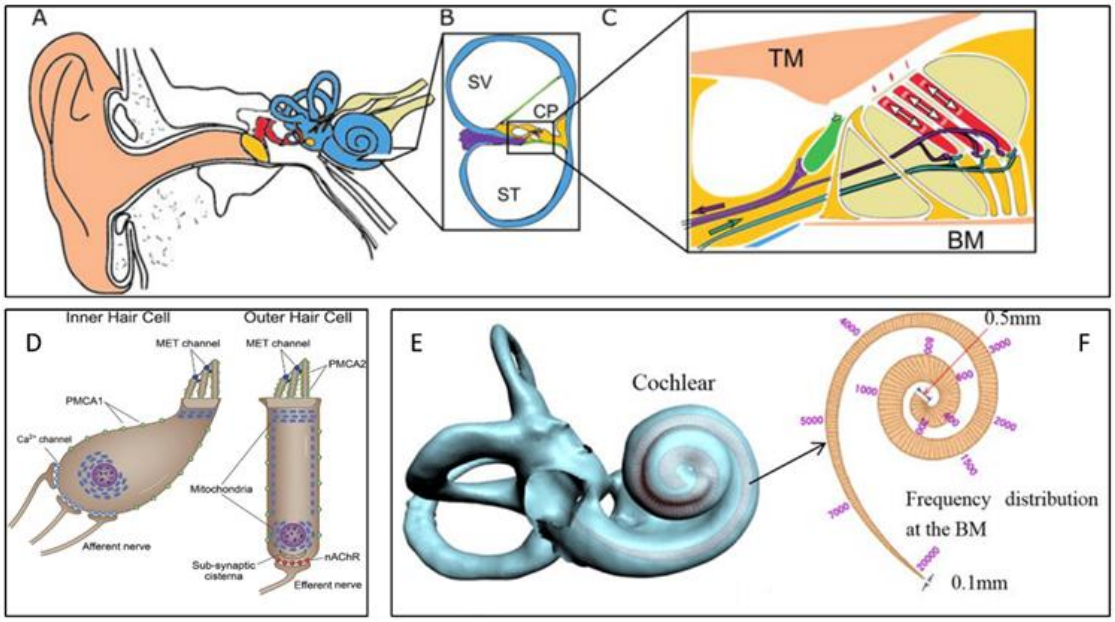

Figure 10 : Cochlea structure. A) the outer (beige), middle (red) and inner (blue) parts of the human ear. B) Cross-section of the cochlea showing the scala vestibuli (SV) and the scala tympani (ST), separated by the cochlear partition (CP) which contains the basilar membrane (BM) and the sensory hair cells (adapted from [240]). These cells are represented in panel C in green (inner hair cells) and red (outer hair cells) and are also reported with more details in

subplot D (adapted from [241]). In panel E a 3D representation of the cochlea is reported and a schematic map of the tonotopic property of the basilar membrane reported in panel F (adapted from [242]).

All these features attracted the interest of researchers working on mechanical and elastic waves manipulation devices, e.g., in the field of structural health monitoring, sensor development, guided waves, etc. There are specific works in the literature that explicitly refer to the cochlea as a bio-inspiration for metamaterial realizations and that propose acoustic rainbow sensors, where the aim is to separate different frequency components into different physical locations along the sensor (see Figure 11 and Refs. [240,242–244]). In particular, the tonotopy and the low amplitude amplifier is reproduced with a set of subwavelength active acoustic graded resonators, coupled to a main propagating waveguide in [240]. Similarly, based on a set of Helmholtz resonators arranged at sub-wavelength intervals along a cochlear-inspired spiral tube in [243], the authors realize an acoustic rainbow trapper, that exploits the frequency selective property of the structure to filter mechanical waves spectrally and spatially to reduce noise and interference in receivers. The tonotopy can be also obtained in a 3D model of the cochlea [242] by grading the mechanical parameters of an helicoidal membrane: in this case the overall cochlear is a local resonant system with the negative dynamic effective mass and stiffness.

Some of the examples of cochlea-inspiration for the design of metamaterials are shown in Figure 11. In particular, in panels A, B, C a gradient-index metamaterial for airborne sounds, made from 38 quarter-wavelength acoustic resonators of different heights is reproduced (from [240]). In panel D a rainbow trapper based on a set of Helmholtz resonators is described (from [243]). In panel E a modal analysis of a helix model of cochlea is reported, showing the different responses to different frequency excitations (in particular, at the top circle, the minimum

natural frequency is 89.3 Hz; (c) at the medial circle is 5000.5 Hz; and at the base circle is 10097.2 Hz).

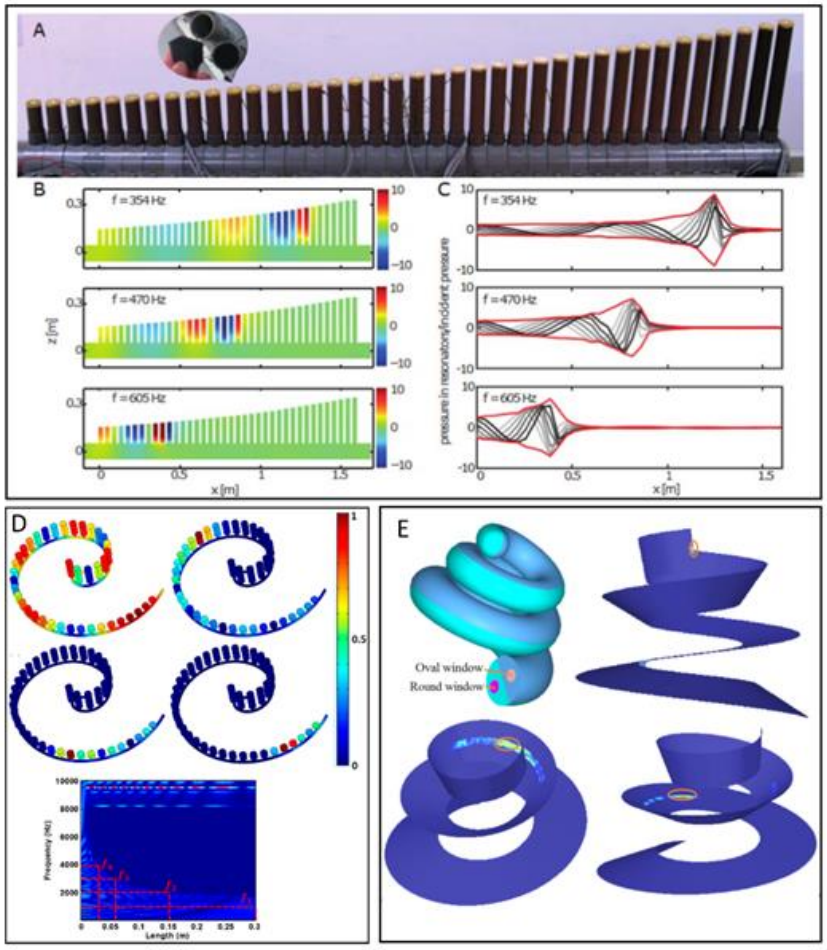

Figure 11 : Metamaterial inspired by the cochlea. Some of the examples of cochlea-inspiration for the design of metamaterials. In particular, in panels A,B,C, a gradient-index metamaterial for airborne sounds, made from 38 quarter-wavelength acoustic resonators of different heights is reproduced (adapted from [240]). In panel D, a rainbow trapper based on a set of Helmholtz resonators is described (adapted from [243]). In panel E, a modal analysis of a helix model of cochlea is reported, showing a different response to different frequency excitations.

5. Natural structural evolution vs. optimization through artificial algorithms

The structures discussed in this review are the result of optimization processes due to natural evolution spanning millions of years. Their common features are summarized in Sections 2.8 and 3.6. These evolutionary processes have however been constrained by the availability of material resources and their fabrication conditions. At the other end of the scale, there are fast developing computational algorithms used in current technology that can be used to optimize artificial materials (often bioinspired) for similar goals, where these boundary conditions can be relaxed or eliminated altogether. In artificial materials, the possibilities of design with different material combinations and distributions are virtually unbounded, and numerical algorithms can be used to optimize specific properties of nature-based architected structures [245]. The use of optimization techniques for the design of periodic structures able to attenuate vibrations, for instance phononic crystals, aims to systematically achieve objectives such as maximizing absolute band gap widths [246], normalized band gap width with respect to their central frequency [247,248], or maximized attenuation per unit length [249]. For each given combination of materials, the objective function must be evaluated through the computation of the band structure of a given unit cell configuration, using various numerical methods [250–252]. A wide variety of optimization techniques to pursue the chosen objective is available in the literature. Among these, topology optimization is one of the most employed and well-developed [253], in combination with algorithms such as Bidirectional Evolutionary Structural Optimization [254]. Another common approach is the use of genetic algorithms, an optimization scheme which is a type of evolutionary algorithm [255] and is well suited for the design of phononic crystals [256]. Another possibility is the use of machine learning tools to design structures which present desirable characteristics, i.e., using an inverse approach [257]. Many of these approaches are being more and more applied in the field of phononics [258]. The types of optimized structures emerging from these algorithms have some common traits with naturally evolved structures, and some distinctive differences. On the one hand, recurring features are

many of those cited in Section 2.8: heterogeneity, porosity, hierarchical organization, efficient resonating structure, graded properties, in some cases chirality [259,260]. In this case, artificial optimization techniques can improve existing bioinspired design for specific objectives. On the other hand, implementing unconstrained numerical optimization can enable a wider exploration of the phase space, potentially leading to exotic designs with little resemblance to existing biological structures. However, this is not surprising, since optimization based on natural evolution is in most cases a muti-objective process, where different properties are simultaneously addressed (e.g., quasistatic strength/toughness and dynamic attenuation).

6. Conclusions

In conclusion, we have presented a review of some notable examples of biological materials exhibiting optimized non-trivial structural architectures to achieve improved vibration control or elastic wave manipulation, for many different purposes. The fields in which these features appear are mainly impact and vibration damping and control, communication, prey detection or mimesis, and sound amplification/focusing. From the documented cases, some recurrent strategies and structural designs emerge. Among them, an important feature is hierarchical structure, which appears to be essential to enable effects at multiple scale levels, and therefore in multiple frequency ranges. Moreover, these recurrent structural features appear at very different size scales (from microns to meters), in disparate environments (terrestrial or marine) and for different functions. This is an indication that the designs are particularly resilient and effective in their purposes, which encourages the adoption of a biomimetic approach to obtain the comparable types of optimized dynamic mechanical properties in artificial structures. This is a particularly attractive proposition in the field of phononic crystals and acoustic metamaterials, which have recently emerged as innovative solutions for wave manipulation and control, and where a biomimetic approach to design has thus far been limited to a few

812 cases, especially considering that biological materials derive from self-assembly, so that are
813 inherently periodic or hierarchical in structure. In general, further investigations in the natural
814 world will no doubt continue to reveal original architectures, designs, and advanced
815 functionalities to be exploited for metamaterials and other vibration-control technologies,
816 where function (or multiple functions) is/are achieved through form and structure.
817

818 **Acknowledgments**

819 All authors are supported by the European Commission H2020 FET Open "Boheme" grant no.
820 863179.

821 **Author contributions**

822 Conceptualization, F.B and N.M.P. All authors contributed to the writing of the manuscript.

823 **Declaration of interests**

824 The authors declare no competing interests.

825 **References**

826 1. Ashby M. *Materials Selection in Mechanical Design: Fourth Edition*. Vol
827 9780080952239.; 2010.
828 2. Ritchie RO. The conflicts between strength and toughness. *Nat Mater*. 2011;10(11).
829 doi:10.1038/nmat3115
830 3. Eisoldt L, Smith A, Scheibel T. Decoding the secrets of spider silk. *Mater Today*.
831 2011;14(3). doi:10.1016/S1369-7021(11)70057-8
832 4. Wolff JO, Paterno GB, Liprandi D, et al. Evolution of aerial spider webs coincided
833 with repeated structural optimization of silk anchorages. *Evolution (N Y)*.
834 2019;73(10):2122-2134. doi:10.1111/evo.13834
835 5. Cranford SW, Tarakanova A, Pugno NM, Buehler MJ. Nonlinear material behaviour
836 of spider silk yields robust webs. *Nature*. 2012;482(7383). doi:10.1038/nature10739
837 6. Wang R, Gupta HS. Deformation and fracture mechanisms of bone and nacre. *Annu*
838 *Rev Mater Res*. 2011;41. doi:10.1146/annurev-matsci-062910-095806
839 7. Gupta HS, Seto J, Wagermaier W, Zaslansky P, Boesecke P, Fratzl P. Cooperative
840 deformation of mineral and collagen in bone at the nanoscale. *Proc Natl Acad Sci U S*
841 *A*. 2006;103(47). doi:10.1073/pnas.0604237103
842 8. Yang W, Chen IH, Gludovatz B, Zimmermann EA, Ritchie RO, Meyers MA. Natural
843 flexible dermal armor. *Adv Mater*. 2013;25(1). doi:10.1002/adma.201202713
844 9. Arndt EM, Moore W, Lee WK, Ortiz C. Mechanistic origins of Bombardier beetle
845 (Brachinini) explosion-induced defensive spray pulsation. *Science (80-)*.
846 2015;348(6234). doi:10.1126/science.1261166
847 10. Yoon SH, Park S. A mechanical analysis of woodpecker drumming and its application
848 to shock-absorbing systems. *Bioinspiration and Biomimetics*. 2011;6(1).
849 doi:10.1088/1748-3182/6/1/016003

11. Sielmann H. *My Year with the Woodpeckers*. Barrie and Rockliff; 1959. https://books.google.it/books?id=jcHRxAEACAAJ.

12. Miniaci M, Krushynska A, Gliozzi AS, Kherraz N, Bosia F, Pugno NM. Design and Fabrication of Bioinspired Hierarchical Dissipative Elastic Metamaterials. *Phys Rev Appl*. 2018;10(2). doi:10.1103/PhysRevApplied.10.024012

13. Li A, Zhao X, Duan G, Anderson S, Zhang X. Diatom Frustule-Inspired Metamaterial Absorbers: The Effect of Hierarchical Pattern Arrays. *Adv Funct Mater*. 2019;29(22). doi:10.1002/adfm.201809029

14. Yan G, Zou HX, Wang S, Zhao LC, Wu ZY, Zhang WM. Bio-inspired vibration isolation: Methodology and design. *Appl Mech Rev*. 2021;73(2). doi:10.1115/1.4049946

15. Patek S, Korff W, Caldwell R. Biomechanics: Deadly strike mechanism of a mantis shrimp. *Nat -LONDON-*. 2004;1(6985).

16. Tadayon M, Amini S, Wang Z, Miserez A. Biomechanical Design of the Mantis Shrimp Saddle: A Biomineralized Spring Used for Rapid Raptorial Strikes. *iScience*. 2018;8. doi:10.1016/j.isci.2018.08.022

17. Tadayon M, Amini S, Masic A, Miserez A. The Mantis Shrimp Saddle: A Biological Spring Combining Stiffness and Flexibility. *Adv Funct Mater*. 2015;25(41). doi:10.1002/adfm.201502987

18. Patek SN, Caldwell RL. Extreme impact and cavitation forces of a biological hammer: Strike forces of the peacock mantis shrimp Odontodactylus scyllarus. *J Exp Biol*. 2005;208(19). doi:10.1242/jeb.01831

19. Weaver JC, Milliron GW, Miserez A, et al. The stomatopod dactyl club: A formidable damage-tolerant biological hammer. *Science (80-)*. 2012;336(6086). doi:10.1126/science.1218764

20. Chua JQI, Srinivasan DV, Idapalapati S, Miserez A. Fracture toughness of the stomatopod dactyl club is enhanced by plastic dissipation: A fracture micromechanics study. *Acta Biomater*. 2021;126. doi:10.1016/j.actbio.2021.03.025

21. Amini S, Tadayon M, Idapalapati S, Miserez A. The role of quasi-plasticity in the extreme contact damage tolerance of the stomatopod dactyl club. *Nat Mater*. 2015;14(9):943-950. doi:10.1038/nmat4309

22. Taylor JRA, Patek SN. Ritualized fighting and biological armor: The impact mechanics of the mantis shrimp's telson. *J Exp Biol*. 2010;213(20). doi:10.1242/jeb.047233

23. Taylor JRA, Scott NI, Rouse GW. Evolution of mantis shrimp telson armour and its role in ritualized fighting. *J R Soc Interface*. 2019;16(157). doi:10.1098/rsif.2019.0203

24. Yaraghi NA, Trikanad AA, Restrepo D, et al. The Stomatopod Telson: Convergent Evolution in the Development of a Biological Shield. *Adv Funct Mater*. 2019. doi:10.1002/adfm.201902238

25. Gibson LJ. Woodpecker pecking: How woodpeckers avoid brain injury. *J Zool*. 2006;270(3). doi:10.1111/j.1469-7998.2006.00166.x

26. Oda J, Sakamoto J, Sakano K. Mechanical evaluation of the skeletal structure and tissue of the woodpecker and its shock absorbing system. *JSME Int Journal, Ser A Solid Mech Mater Eng*. 2006;49(3). doi:10.1299/jsmea.49.390

27. Wang L, CheungJason JTM, Pu F, Li D, Zhang M, Fan Y. Why do woodpeckers resist head impact injury: A biomechanical investigation. *PLoS One*. 2011;6(10). doi:10.1371/journal.pone.0026490

28. Liu YZ, Qiu XM, Ma HL, Fu WW, Yu TX. A study of woodpecker's pecking process and the impact response of its brain. *Int J Impact Eng*. 2017;108. doi:10.1016/j.ijimpeng.2017.05.016

29. Wu CW, Zhu ZD, Zhang W. How woodpecker avoids brain injury? In: *Journal of Physics: Conference Series*. Vol 628. ; 2015. doi:10.1088/1742-6596/628/1/012007

30. Zhu ZD, Ma GJ, Wu CW, Chen Z. Numerical study of the impact response of woodpecker's head. *AIP Adv*. 2012;2(4). doi:10.1063/1.4770305

31. Zhu Z, Wu C, Zhang W. Frequency analysis and anti-shock mechanism of woodpecker's head structure. *J Bionic Eng*. 2014;11(2). doi:10.1016/S1672-6529(14)60045-7

32. Zhu Z, Zhang W, Wu C. Energy conversion in woodpecker on successive peckings and its role on anti-shock protection of brain. *Sci China Technol Sci*. 2014;57(7). doi:10.1007/s11431-014-5582-5

33. Lee N, Horstemeyer MF, Rhee H, Nabors B, Liao J, Williams LN. Hierarchical multiscale structure - Property relationships of the red-bellied woodpecker (Melanerpes carolinus) beak. *J R Soc Interface*. 2014;11(96). doi:10.1098/rsif.2014.0274

34. Jung JY, Naleway SE, Yaraghi NA, et al. Structural analysis of the tongue and hyoid apparatus in a woodpecker. *Acta Biomater*. 2016;37. doi:10.1016/j.actbio.2016.03.030

35. Li Y, Zhang W, Meng QL, Jiang G, Wu CW. How woodpecker protects its brain from concussion during pecking compared with chicken and pigeon. *AIP Adv*. 2020;10(6). doi:10.1063/5.0004546

36. Raut MS, Gopalakrishnan S. Elastic and viscoelastic flexural wave motion in woodpecker-beak-inspired structures. *Bioinspir Biomim*. 2021. doi:10.1088/1748-3190/abf745

37. Garland AP, Adstedt KM, Casias ZJ, et al. Coulombic friction in metamaterials to dissipate mechanical energy. *Extrem Mech Lett*. 2020;40. doi:10.1016/j.eml.2020.100847

38. Mayer G. Rigid biological systems as models for synthetic composites. *Science (80-)*. 2005;310(5751). doi:10.1126/science.1116994

39. Yourdkhani M, Pasini D, Barthelat F. The hierarchical structure of seashells optimized to resist mechanical threats. *WIT Trans Ecol Environ*. 2010;138. doi:10.2495/DN100131

40. Barthelat F, Tang H, Zavattieri PD, Li CM, Espinosa HD. On the mechanics of mother-of-pearl: A key feature in the material hierarchical structure. *J Mech Phys Solids*. 2007;55(2). doi:10.1016/j.jmps.2006.07.007

41. Sarikaya M, Aksay IA. Biomimetics : design and processing of materials. *AIP Ser Polym complex Mater*. 1995.

42. Meyers MA, Lin AYM, Chen PY, Muyco J. Mechanical strength of abalone nacre: Role of the soft organic layer. *J Mech Behav Biomed Mater*. 2008;1(1). doi:10.1016/j.jmbbm.2007.03.001

43. Barthelat F, Yin Z, Buehler MJ. Structure and mechanics of interfaces in biological materials. *Nat Rev Mater*. 2016;1. doi:10.1038/natrevmats.2016.7

44. Krauss S, Monsonego-Ornan E, Zelzer E, Fratzl P, Shahar R. Mechanical function of a complex three-dimensional suture joining the bony elements in the shell of the red-eared slider turtle. *Adv Mater*. 2009;21(4). doi:10.1002/adma.200801256

45. Damiens R, Rhee H, Hwang Y, et al. Compressive behavior of a turtle's shell: Experiment, modeling, and simulation. *J Mech Behav Biomed Mater*. 2012;6. doi:10.1016/j.jmbbm.2011.10.011

46. Yang W, Naleway SE, Porter MM, Meyers MA, McKittrick J. The armored carapace of the boxfish. *Acta Biomater*. 2015;23. doi:10.1016/j.actbio.2015.05.024

47. PRITCHARD JJ, SCOTT JH, GIRGIS FG. The structure and development of cranial and facial sutures. *J Anat*. 1956;90(1).

950 48. Gao C, Hasseldine BPJ, Li L, Weaver JC, Li Y. Amplifying Strength, Toughness, and
951 Auxeticity via Wavy Sutural Tessellation in Plant Seedcoats. *Adv Mater*. 2018;30(36).
952 doi:10.1002/adma.201800579
953 49. Lu H, Zhang J, Wu N, Liu KB, Xu D, Li Q. Phytoliths analysis for the discrimination
954 of Foxtail millet (Setaria italica) and Common millet (Panicum miliaceum). *PLoS One*.
955 2009;4(2). doi:10.1371/journal.pone.0004448
956 50. Gebeshuber IC, Kindt JH, Thompson JB, et al. Atomic force microscopy study of
957 living diatoms in ambient conditions. *J Microsc*. 2003;212(3). doi:10.1111/j.1365-
958 2818.2003.01275.x
959 51. Li Y, Ortiz C, Boyce MC. Bioinspired, mechanical, deterministic fractal model for
960 hierarchical suture joints. *Phys Rev E - Stat Nonlinear, Soft Matter Phys*. 2012;85(3).
961 doi:10.1103/PhysRevE.85.031901
962 52. Jaslow CR, Biewener AA. Strain patterns in the horncores, cranial bones and sutures
963 of goats (Capra hircus) during impact loading. *J Zool*. 1995;235(2).
964 doi:10.1111/j.1469-7998.1995.tb05137.x
965 53. Jaslow CR. Mechanical properties of cranial sutures. *J Biomech*. 1990;23(4).
966 doi:10.1016/0021-9290(90)90059-C
967 54. Li Y, Ortiz C, Boyce MC. A generalized mechanical model for suture interfaces of
968 arbitrary geometry. *J Mech Phys Solids*. 2013;61(4). doi:10.1016/j.jmps.2012.10.004
969 55. Yu Z, Liu J, Wei X. Achieving outstanding damping performance through bio-inspired
970 sutural tessellations. *J Mech Phys Solids*. 2020;142. doi:10.1016/j.jmps.2020.104010
971 56. Gao C, Slesarenko V, Boyce MC, Rudykh S, Li Y. Instability-Induced Pattern
972 Transformation in Soft Metamaterial with Hexagonal Networks for Tunable Wave
973 Propagation. *Sci Rep*. 2018;8(1). doi:10.1038/s41598-018-30381-1
974 57. Ghazlan A, Ngo TD, Tran P. Influence of interfacial geometry on the energy

absorption capacity and load sharing mechanisms of nacreous composite shells. *Compos Struct*. 2015;132. doi:10.1016/j.compstruct.2015.05.045

58. Gao C, Li Y. Mechanical model of bio-inspired composites with sutural tessellation. *J Mech Phys Solids*. 2019;122. doi:10.1016/j.jmps.2018.09.015

59. Jasinoski SC, Reddy BD, Louw KK, Chinsamy A. Mechanics of cranial sutures using the finite element method. *J Biomech*. 2010;43(16). doi:10.1016/j.jbiomech.2010.08.007

60. Chen IH, Yang W, Meyers MA. Leatherback sea turtle shell: A tough and flexible biological design. *Acta Biomater*. 2015;28. doi:10.1016/j.actbio.2015.09.023

61. De Blasio FV. The role of suture complexity in diminishing strain and stress in ammonoid phragmocones. *Lethaia*. 2008;41(1). doi:10.1111/j.1502-3931.2007.00037.x

62. Pérez-Claros JA, Palmqvist P, Olóriz F. First and second orders of suture complexity in ammonites: A new methodological approach using fractal analysis. *Math Geol*. 2002;34(3). doi:10.1023/A:1014847007351

63. Studart AR. Towards high-performance bioinspired composites. *Adv Mater*. 2012;24(37). doi:10.1002/adma.201201471

64. Currey JD. *Bones: Structure and Mechanics*. Vol 9781400849505.; 2013. doi:10.1016/s0021-9290(03)00033-2

65. Sullivan TN, Wang B, Espinosa HD, Meyers MA. Extreme lightweight structures: avian feathers and bones. *Mater Today*. 2017;20(7). doi:10.1016/j.mattod.2017.02.004

66. Qwamizadeh M, Liu P, Zhang Z, Zhou K, Wei Zhang Y. Hierarchical Structure Enhances and Tunes the Damping Behavior of Load-Bearing Biological Materials. *J Appl Mech Trans ASME*. 2016;83(5). doi:10.1115/1.4032861

67. Lazarus BS, Velasco-Hogan A, Gómez-del Río T, Meyers MA, Jasiuk I. A review of

impact resistant biological and bioinspired materials and structures. *J Mater Res Technol*. 2020;9(6). doi:10.1016/j.jmrt.2020.10.062

68. Libonati F, Buehler MJ. Advanced Structural Materials by Bioinspiration. *Adv Eng Mater*. 2017;19(5). doi:10.1002/adem.201600787

69. Evans JA, Tavakoli MB. Ultrasonic attenuation and velocity in bone. *Phys Med Biol*. 1990;35(10). doi:10.1088/0031-9155/35/10/004

70. Lakes R, Yoon HS, Lawrence Katz J. Ultrasonic wave propagation and attenuation in wet bone. *J Biomed Eng*. 1986;8(2). doi:10.1016/0141-5425(86)90049-X

71. Haïat G, Padilla F, Peyrin F, Laugier P. Fast wave ultrasonic propagation in trabecular bone: Numerical study of the influence of porosity and structural anisotropy. *J Acoust Soc Am*. 2008;123(3). doi:10.1121/1.2832611

72. Bochud N, Vallet Q, Minonzio JG, Laugier P. Predicting bone strength with ultrasonic guided waves. *Sci Rep*. 2017;7. doi:10.1038/srep43628

73. Panteliou SD, Xirafaki AL, Panagiotopoulos E, Varakis JN, Vagenas N V., Kontoyannis CG. Modal damping for monitoring bone integrity and osteoporosis. *J Biomech Eng*. 2004;126(1). doi:10.1115/1.1644561

74. Michimoto I, Miyashita K, Suzuyama H, et al. Simulation study on the effects of cancellous bone structure in the skull on ultrasonic wave propagation. *Sci Rep*. 2021;11(1). doi:10.1038/s41598-021-96502-5

75. Neupetsch C, Hensel E, Werner M, et al. Development and Validation of Bone Models using Structural Dynamic Measurement Methods. *Curr Dir Biomed Eng*. 2019;5(1). doi:10.1515/cdbme-2019-0086

76. Kadic M, Milton GW, van Hecke M, Wegener M. 3D metamaterials. *Nat Rev Phys*. 2019;1(3). doi:10.1038/s42254-018-0018-y

77. Meza LR, Phlipot GP, Portela CM, et al. Reexamining the mechanical property space

of three-dimensional lattice architectures. *Acta Mater*. 2017;140. doi:10.1016/j.actamat.2017.08.052

78. Arretche I, Matlack KH. Experimental Testing of Vibration Mitigation in 3D-Printed Architected Metastructures. *J Appl Mech*. 2019;86(11). doi:10.1115/1.4044135

79. Zelhofer AJ, Kochmann DM. On acoustic wave beaming in two-dimensional structural lattices. *Int J Solids Struct*. 2017;115-116. doi:10.1016/j.ijsolstr.2017.03.024

80. Aguirre TG, Fuller L, Ingrole A, et al. Bioinspired material architectures from bighorn sheep horncore velar bone for impact loading applications. *Sci Rep*. 2020;10(1). doi:10.1038/s41598-020-76021-5

81. Jones H. Introduction to Solid State Physics by C. Kittel . *Acta Crystallogr*. 1957;10(5). doi:10.1107/s0365110x57001280

82. Stratigaki V, Manca E, Prinos P, et al. Large-scale experiments on wave propagation over Posidonia oceanica. *J Hydraul Res*. 2011;49(SUPPL.1). doi:10.1080/00221686.2011.583388

83. Novi L. A numerical model for high resolution simulations of marine fluid dynamics and coastal morphodynamics. *PhD Thesis, Univ Pisa*. 2019.

84. Alberello, A.; Bennetts, L.; Onorato, M; Vichi, M; MacHutchon, K; Eayrs, C; Ntamba Ntamba, B; Benetazzo, A; Bergamasco, F; Nelli, F; Pattani, R; Clarke, H; Tersigni, I; Toffoli A. Three-dimensional imaging of waves and floe sizes in the marginal ice zone during an explosive cyclone. *Accept Publ Nat Commun*. 2022.

85. Lott M, Roux P, Garambois S, Guéguen P, Colombi A. Evidence of metamaterial physics at the geophysics scale: The METAFORET experiment. *Geophys J Int*. 2020;220(2). doi:10.1093/gji/ggz528

86. Moore JR, Maguire DA. Natural sway frequencies and damping ratios of trees: Concepts, review and synthesis of previous studies. *Trees - Struct Funct*. 2004;18(2).

doi:10.1007/s00468-003-0295-6

87. Masters WM, Markl H. Vibration signal transmission in spider orb webs. *Science (80-)*. 1981;213(4505). doi:10.1126/science.213.4505.363

88. Eberhard W. Spider Webs. In: University of Chicago Press; 2020:24-74. doi:doi:10.7208/9780226534749-002

89. Asakura T, Miller T. *Biotechnology of Silk*.; 2014.

90. Basu A. *Advances in Silk Science and Technology*.; 2015. doi:10.1016/C2014-0-02586-5

91. Rising A, Johansson J. Toward spinning artificial spider silk. *Nat Chem Biol*. 2015;11(5). doi:10.1038/nchembio.1789

92. Andersson M, Jia Q, Abella A, et al. Biomimetic spinning of artificial spider silk from a chimeric minispidroin. *Nat Chem Biol*. 2017;13(3). doi:10.1038/nchembio.2269

93. Greco G, Pantano MF, Mazzolai B, Pugno NM. Imaging and mechanical characterization of different junctions in spider orb webs. *Sci Rep*. 2019;9(1). doi:10.1038/s41598-019-42070-8

94. Agnarsson I, Kuntner M, Blackledge TA. Bioprospecting finds the toughest biological material: Extraordinary silk from a giant riverine orb spider. *PLoS One*. 2010;5(9). doi:10.1371/journal.pone.0011234

95. Yu H, Yang J, Sun Y. Energy Absorption of Spider Orb Webs During Prey Capture: A Mechanical Analysis. *J Bionic Eng*. 2015;12(3). doi:10.1016/S1672-6529(14)60136-0

96. Sensenig AT, Lorentz KA, Kelly SP, Blackledge TA. Spider orb webs rely on radial threads to absorb prey kinetic energy. *J R Soc Interface*. 2012;9(73). doi:10.1098/rsif.2011.0851

97. Guo Y, Chang Z, Guo HY, et al. Synergistic adhesion mechanisms of spider capture silk. *J R Soc Interface*. 2018;15(140). doi:10.1098/rsif.2017.0894

98. Sahni V, Blackledge TA, Dhinojwala A. Changes in the adhesive properties of spider aggregate glue during the evolution of cobwebs. *Sci Rep*. 2011;1. doi:10.1038/srep00041

99. Grawe I, Wolff JO, Gorb SN. Composition and substrate-dependent strength of the silken attachment discs in spiders. *J R Soc Interface*. 2014;11(98):20140477-20140477. doi:10.1098/rsif.2014.0477

100. Wolff JO, Herberstein ME. Three-dimensional printing spiders: Back-and-forth glue application yields silk anchorages with high pull-off resistance under varying loading situations. *J R Soc Interface*. 2017. doi:10.1098/rsif.2016.0783

101. Meyer A, Pugno NM, Cranford SW. Compliant threads maximize spider silk connection strength and toughness. *J R Soc Interface*. 2014;11(98). doi:10.1098/rsif.2014.0561

102. Zhu Q, Tang X, Feng S, Zhong Z, Yao J, Yao Z. ZIF-8@SiO2 composite nanofiber membrane with bioinspired spider web-like structure for efficient air pollution control. *J Memb Sci*. 2019;581. doi:10.1016/j.memsci.2019.03.075

103. Xu B, Yang Y, Yan Y, Zhang B. Bionics design and dynamics analysis of space webs based on spider predation. *Acta Astronaut*. 2019;159. doi:10.1016/j.actaastro.2019.03.045

104. Vollrath F, Krink T. Spider webs inspiring soft robotics. *J R Soc Interface*. 2020;17(172). doi:10.1098/rsif.2020.0569

105. Lin LH, Edmonds DT, Vollrath F. Structural engineering of an orb-spider's web. *Nature*. 1995;373(6510). doi:10.1038/373146a0

106. Kawano A, Morassi A. Can the spider hear the position of the prey? *Mech Syst Signal Process*. 2020;143. doi:10.1016/j.ymssp.2020.106838

107. Das R, Kumar A, Patel A, Vijay S, Saurabh S, Kumar N. Biomechanical

characterization of spider webs. *J Mech Behav Biomed Mater*. 2017;67. doi:10.1016/j.jmbbm.2016.12.008

108. Masters WM. Vibrations in the orbwebs of Nuctenea sclopetaria (Araneidae). *Behav Ecol Sociobiol*. 1984. doi:10.1007/bf00292978

109. Landolfa MA, Barth FG. Vibrations in the orb web of the spider Nephila clavipes: Cues for discrimination and orientation. *J Comp Physiol - A Sensory, Neural, Behav Physiol*. 1996;179(4). doi:10.1007/BF00192316

110. Klärner D, Barth FG. Vibratory signals and prey capture in orb-weaving spiders (Zygiella x-notata, Nephila clavipes; Araneidae). *J Comp Physiol □ A*. 1982. doi:10.1007/BF00619783

111. Main IG. *Vibrations and Waves in Physics*. Cambridge University Press; 1993. doi:10.1017/CBO9781139170567

112. Mortimer B, Holland C, Windmill JFC, Vollrath F. Unpicking the signal thread of the sector web spider Zygiella x-notata. *J R Soc Interface*. 2015;12(113). doi:10.1098/rsif.2015.0633

113. Mortimer B, Soler A, Siviour CR, Zaera R, Vollrath F. Tuning the instrument: Sonic properties in the spider's web. *J R Soc Interface*. 2016;13(122). doi:10.1098/rsif.2016.0341

114. Wirth E, Barth FG. Forces in the spider orb web. *J Comp Physiol A*. 1992. doi:10.1007/BF00223966

115. Watanabe T. Web tuning of an orb-web spider, Octonoba sybotides, regulated prey-catching behaviour. *Proc R Soc B Biol Sci*. 2000;267(1443). doi:10.1098/rspb.2000.1038

116. Yang T, Xu S, Kaewunruen S. Nonlinear free vibrations of spider web structures. In: *Proceedings of the 26th International Congress on Sound and Vibration, ICSV 2019*. ;

2019.

117. Kaewunruen S, Ngamkhanong C, Xu S. Large amplitude vibrations of imperfect spider web structures. *Sci Rep*. 2020;10(1). doi:10.1038/s41598-020-76269-x

118. Drodge DR, Mortimer B, Holland C, Siviour CR. Ballistic impact to access the high-rate behaviour of individual silk fibres. *J Mech Phys Solids*. 2012;60(10). doi:10.1016/j.jmps.2012.06.007

119. Boutry C, Blackledge TA. Evolution of supercontraction in spider silk: Structure-function relationship from tarantulas to orb-weavers. *J Exp Biol*. 2010. doi:10.1242/jeb.046110

120. Boutry C, Blackledge TA. Wet webs work better: Humidity, supercontraction and the performance of spider orb webs. *J Exp Biol*. 2013;216(19). doi:10.1242/jeb.084236

121. Elices M, Plaza GR, Pérez-Rigueiro J, Guinea G V. The hidden link between supercontraction and mechanical behavior of spider silks. *J Mech Behav Biomed Mater*. 2011;4(5). doi:10.1016/j.jmbbm.2010.09.008

122. Liu Y, Shao Z, Vollrath F. Relationships between supercontraction and mechanical properties of spider silk. *Nat Mater*. 2005;4(12). doi:10.1038/nmat1534

123. Yazawa K, Malay AD, Masunaga H, Norma-Rashid Y, Numata K. Simultaneous effect of strain rate and humidity on the structure and mechanical behavior of spider silk. *Commun Mater*. 2020;1(1). doi:10.1038/s43246-020-0011-8

124. Mortimer B, Gordon SD, Holland C, Siviour CR, Vollrath F, Windmill JFC. The speed of sound in silk: Linking material performance to biological function. *Adv Mater*. 2014;26(30). doi:10.1002/adma.201401027

125. Frohlich C, Buskirk RE. Transmission and attenuation of vibration in orb spider webs. *J Theor Biol*. 1982;95(1). doi:10.1016/0022-5193(82)90284-3

126. Vollrath F, Selden P. The role of behavior in the evolution of spiders, silks, and webs.

Annu Rev Ecol Evol Syst. 2007. doi:10.1146/annurev.ecolsys.37.091305.110221

127. Miniaci M, Krushynska A, Movchan AB, Bosia F, Pugno NM. Spider web-inspired acoustic metamaterials. *Appl Phys Lett*. 2016. doi:10.1063/1.4961307

128. Sepehri S, Jafari H, Mashhadi MM, Yazdi MRH, Fakhrabadi MMS. Study of tunable locally resonant metamaterials: Effects of spider-web and snowflake hierarchies. *Int J Solids Struct*. 2020;204-205. doi:10.1016/j.ijsolstr.2020.08.014

129. Dal Poggetto VF, Bosia F, Miniaci M, Pugno NM. Optimization of spider web-inspired phononic crystals to achieve tailored dispersion for diverse objectives. *Mater Des*. 2021;209. doi:10.1016/j.matdes.2021.109980

130. Krushynska AO, Bosia F, Miniaci M, Pugno NM. Spider web-structured labyrinthine acoustic metamaterials for low-frequency sound control. *New J Phys*. October 2017. doi:10.1088/1367-2630/aa83f3

131. Huang H, Cao E, Zhao M, Alamri S, Li B. Spider web-inspired lightweight membrane-type acoustic metamaterials for broadband low-frequency sound isolation. *Polymers (Basel)*. 2021. doi:10.3390/polym13071146

132. Ganske AS, Uhl G. The sensory equipment of a spider – A morphological survey of different types of sensillum in both sexes of Argiope bruennichi (Araneae, Araneidae). *Arthropod Struct Dev*. 2018;47(2). doi:10.1016/j.asd.2018.01.001

133. Barth FG. Spider mechanoreceptors. *Curr Opin Neurobiol*. 2004;14(4). doi:10.1016/j.conb.2004.07.005

134. Seo JH, Kim KJ, Kim H, Moon MJ. Lyriform vibration receptors in the web-building spider, Nephila clavata (Araneidae: Araneae: Arachnida). *Entomol Res*. 2020;50(12). doi:10.1111/1748-5967.12470

135. Barth FG. A spider in motion: facets of sensory guidance. *J Comp Physiol A Neuroethol Sensory, Neural, Behav Physiol*. 2021;207(2). doi:10.1007/s00359-020-

01449-z

136. Klopsch C, Kuhlmann HC, Barth FG. Airflow elicits a spider's jump towards airborne prey. I. Airflow around a flying blowfly. *J R Soc Interface*. 2012;9(75). doi:10.1098/rsif.2012.0186

137. Klopsch C, Kuhlmann HC, Barth FG. Airflow elicits a spider's jump towards airborne prey. II. Flow characteristics guiding behaviour. *J R Soc Interface*. 2013;10(82). doi:10.1098/rsif.2012.0820

138. Bathellier B, Barth FG, Albert JT, Humphrey JAC. Viscosity-mediated motion coupling between pairs of trichobothria on the leg of the spider Cupiennius salei. *J Comp Physiol A Neuroethol Sensory, Neural, Behav Physiol*. 2005;191(8). doi:10.1007/s00359-005-0629-5

139. Guarino R, Greco G, Mazzolai B, Pugno NM. Fluid-structure interaction study of spider's hair flow-sensing system. In: *Materials Today: Proceedings*. Vol 7. ; 2019. doi:10.1016/j.matpr.2018.11.104

140. Young SL, Chyasnavichyus M, Erko M, et al. A spider's biological vibration filter: Micromechanical characteristics of a biomaterial surface. *Acta Biomater*. 2014;10(11). doi:10.1016/j.actbio.2014.07.023

141. Erko M, Younes-Metzler O, Rack A, et al. Micro- and nano-structural details of a spider's filter for substrate vibrations: Relevance for low-frequency signal transmission. *J R Soc Interface*. 2015;12(104). doi:10.1098/rsif.2014.1111

142. Dal Poggetto, V.F., Bosia, F., Greco, G., Pugno NM. Prey Impact Localization Enabled by Material and Structural Interaction in Spider Orb Webs. *Adv Theory Simulations*. 2022:2100282. doi:10.1002/adts.202100282

143. Dijkstra M, Van Baar JJ, Wiegerink RJ, Lammerink TSJ, De Boer JH, Krijnen GJM. Artificial sensory hairs based on the flow sensitive receptor hairs of crickets. *J*

Micromechanics Microengineering. 2005;15(7). doi:10.1088/0960-1317/15/7/019

144. Wu Z, Ai J, Ma Z, et al. Flexible Out-of-Plane Wind Sensors with a Self-Powered Feature Inspired by Fine Hairs of the Spider. *ACS Appl Mater Interfaces*. 2019;11(47). doi:10.1021/acsami.9b15382

145. Chen N, Tucker C, Engel JM, Yang Y, Pandya S, Liu C. Design and characterization of artificial haircell sensor for flow sensing with ultrahigh velocity and angular sensitivity. *J Microelectromechanical Syst*. 2007;16(5). doi:10.1109/JMEMS.2007.902436

146. Kang D, Pikhitsa P V., Choi YW, et al. Ultrasensitive mechanical crack-based sensor inspired by the spider sensory system. *Nature*. 2014;516(7530). doi:10.1038/nature14002

147. Kim T, Lee T, Lee G, et al. Polyimide encapsulation of spider-inspired crack-based sensors for durability improvement. *Appl Sci*. 2018;8(3). doi:10.3390/app8030367

148. Zhou J, Miles RN. Sensing fluctuating airflow with spider silk. *Proc Natl Acad Sci U S A*. 2017;114(46). doi:10.1073/pnas.1710559114

149. Stockmann R. Introduction to scorpion biology and ecology. In: *Scorpion Venoms*. ; 2015. doi:10.1007/978-94-007-6404-0_14

150. O'Connell-Rodwell CE. Keeping an "ear" to the ground: Seismic communication in elephants. *Physiology*. 2007. doi:10.1152/physiol.00008.2007

151. Narins PM, Reichman OJ, Jarvis JUM, Lewis ER. Seismic signal transmission between burrows of the Cape mole-rat, Georychus capensis. *J Comp Physiol A*. 1992. doi:10.1007/BF00190397

152. Brownell PH. Compressional and surface waves in sand: Used by desert scorpions to locate prey. *Science (80-)*. 1977. doi:10.1126/science.197.4302.479

153. Brownell PH. Prey Detection by the Sand Scorpion. *Sci Am*. 1984.

doi:10.1038/scientificamerican1284-86

154. French AS, Torkkeli PH. Mechanotransduction in spider slit sensilla. In: *Canadian Journal of Physiology and Pharmacology*. ; 2004. doi:10.1139/y04-031

155. Mineo MF, Del Claro K. Mechanoreceptive function of pectines in the Brazilian yellow scorpion Tityus serrulatus: Perception of substrate-borne vibrations and prey detection. *Acta Ethol*. 2006. doi:10.1007/s10211-006-0021-7

156. Brownell P, Farley RD. Orientation to vibrations in sand by the nocturnal scorpion Paruroctonus mesaensis: Mechanism of target localization. *J Comp Physiol □ A*. 1979. doi:10.1007/BF00613081

157. Brownell P, Farley RD. Prey-localizing behaviour of the nocturnal desert scorpion, Paruroctonus mesaensis: Orientation to substrate vibrations. *Anim Behav*. 1979. doi:10.1016/0003-3472(79)90138-6

158. Brownell PH, Van Leo Hemmen J. Vibration sensitivity and a computational theory for prey-localizing behavior in sand scorpions'. *Am Zool*. 2001. doi:10.1093/icb/41.5.1229

159. Wang K, Zhang J, Liu L, et al. Vibrational Receptor of Scorpion (Heterometrus petersii): The Basitarsal Compound Slit Sensilla. *J Bionic Eng*. 2019;16(1). doi:10.1007/s42235-019-0008-5

160. Fratzl P, Kolednik O, Fischer FD, Dean MN. The mechanics of tessellations-bioinspired strategies for fracture resistance. *Chem Soc Rev*. 2016. doi:10.1039/c5cs00598a

161. Fratzl P, Barth FG. Biomaterial systems for mechanosensing and actuation. *Nature*. 2009. doi:10.1038/nature08603

162. González-Santillán E, Prendini L. Redefinition and generic revision of the north american vaejovid scorpion subfamily syntropinae kraepelin, 1905, with descriptions

of six new genera. *Bull Am Museum Nat Hist*. 2013;(382). doi:10.1206/830.1

163. Hill PSM. How do animals use substrate-borne vibrations as an information source? *Naturwissenschaften*. 2009;96(12). doi:10.1007/s00114-009-0588-8

164. Mortimer B, Rees WL, Koelemeijer P, Nissen-Meyer T. Classifying elephant behaviour through seismic vibrations. *Curr Biol*. 2018;28(9). doi:10.1016/j.cub.2018.03.062

165. Reinwald M, Moseley B, Szenicer A, et al. Seismic localization of elephant rumbles as a monitoring approach. *J R Soc Interface*. 2021;18(180). doi:10.1098/rsif.2021.0264

166. Mortimer B, Walker JA, Lolchuragi DS, Reinwald M, Daballen D. Noise matters: Elephants show risk-avoidance behaviour in response to human-generated seismic cues. *Proc R Soc B Biol Sci*. 2021;288(1953). doi:10.1098/rspb.2021.0774

167. Eaton TH, Cott HB. Adaptive Coloration in Animals. *Am Midl Nat*. 1940;24(3). doi:10.2307/2420875

168. Fenton MB. Predator-Prey Interactions: Co-evolution between Bats and Their Prey . Springer Briefs in Animal Sciences. By David Steve Jacobs and Anna Bastian. Cham (Switzerland) and New York: Springer. $54.99 (paper); $39.99 (ebook). xi + 135 p.; ill.; index and index of species. ISBN: 978-3-319-32490-6 (pb); 978-3-319-32492-0 (eb). 2016. . *Q Rev Biol*. 2018;93(2). doi:10.1086/698066

169. McClure M, Clerc C, Desbois C, et al. Why has transparency evolved in aposematic butterflies? Insights from the largest radiation of aposematic butterflies, the Ithomiini. *Proc R Soc B Biol Sci*. 2019;286(1901). doi:10.1098/rspb.2018.2769

170. Rubin JJ, Hamilton CA, McClure CJW, Chadwell BA, Kawahara AY, Barber JR. The evolution of anti-bat sensory illusions in moths. *Sci Adv*. 2018;4(7). doi:10.1126/sciadv.aar7428

171. Vamosi SM. On the role of enemies in divergence and diversification of prey: A

review and synthesis. *Can J Zool*. 2005;83(7). doi:10.1139/z05-063

172. Kelley LA, Kelley JL. Animal visual illusion and confusion: The importance of a perceptual perspective. *Behav Ecol*. 2014;25(3). doi:10.1093/beheco/art118

173. Miller LA, Surlykke A. How some insects detect and avoid being eaten by bats: Tactics and countertactics of prey and predator. *Bioscience*. 2001;51(7). doi:10.1641/0006-3568(2001)051[0570:HSIDAA]2.0.CO;2

174. Corcoran AJ, Hristov NI. Convergent evolution of anti-bat sounds. *J Comp Physiol A Neuroethol Sensory, Neural, Behav Physiol*. 2014;200(9). doi:10.1007/s00359-014-0924-0

175. Corcoran AJ, Barber JR, Conner WE. Tiger moth jams bat sonar. *Science (80-).* 2009;325(5938). doi:10.1126/science.1174096

176. Shen Z, Neil TR, Robert D, Drinkwater BW, Holderied MW. Biomechanics of a moth scale at ultrasonic frequencies. *Proc Natl Acad Sci U S A*. 2018;115(48). doi:10.1073/pnas.1810025115

177. O'Reilly LJ, Agassiz DJL, Neil TR, Holderied MW. Deaf moths employ acoustic Müllerian mimicry against bats using wingbeat-powered tymbals. *Sci Rep*. 2019;9(1). doi:10.1038/s41598-018-37812-z

178. Zeng J, Xiang N, Jiang L, et al. Moth wing scales slightly increase the absorbance of bat echolocation calls. *PLoS One*. 2011;6(11). doi:10.1371/journal.pone.0027190

179. Neil TR, Shen Z, Robert D, Drinkwater BW, Holderied MW. Moth wings are acoustic metamaterials. *Proc Natl Acad Sci U S A*. 2020;117(49). doi:10.1073/pnas.2014531117

180. Neil TR, Shen Z, Robert D, Drinkwater BW, Holderied MW. Thoracic scales of moths as a stealth coating against bat biosonar. *J R Soc Interface*. 2020;17(163). doi:10.1098/rsif.2019.0692

181. Barber JR, Leavell BC, Keener AL, et al. Moth tails divert bat attack: Evolution of acoustic deflection. *Proc Natl Acad Sci U S A*. 2015;112(9). doi:10.1073/pnas.1421926112

182. Wohlgemuth MJ, Luo J, Moss CF. Three-dimensional auditory localization in the echolocating bat. *Curr Opin Neurobiol*. 2016;41. doi:10.1016/j.conb.2016.08.002

183. Arenas JP, Crocker MJ. Recent trends in porous sound-absorbing materials. *Sound Vib*. 2010;44(7).

184. Conner WE. Adaptive Sounds and Silences: Acoustic Anti-Predator Strategies in Insects. In: ; 2014. doi:10.1007/978-3-642-40462-7_5

185. HEGEL JR, CASEY TM. Thermoregulation and Control of Head Temperature in the Sphinx Moth, Manduca Sexta . *J Exp Biol*. 1982;101(1). doi:10.1242/jeb.101.1.1

186. Lee W-J, Moss CF. Can the elongated hindwing tails of fluttering moths serve as false sonar targets to divert bat attacks? *J Acoust Soc Am*. 2016;139(5). doi:10.1121/1.4947423

187. Kirchner WH. Acoustical communication in honeybees. *Apidologie*. 1993. doi:10.1051/apido:19930309

188. Ono M, Igarashi T, Ohno E, Sasaki M. Unusual thermal defence by a honeybee against mass attack by hornets. *Nature*. 1995. doi:10.1038/377334a0

189. Ugajin A, Kiya T, Kunieda T, Ono M, Yoshida T, Kubo T. Detection of neural activity in the brains of japanese honeybee workers during the formation of a "Hot defensive bee ball." *PLoS One*. 2012. doi:10.1371/journal.pone.0032902

190. Schaber CF, Gorb SN, Barth FG. Force transformation in spider strain sensors: White light interferometry. *J R Soc Interface*. 2012;9(71). doi:10.1098/rsif.2011.0565

191. Greco G, Mirbaha H, Schmuck B, Rising A, Pugno NM. Artificial and natural silk materials have high mechanical property variability regardless of sample size. *Sci Rep*.

2022;12(1). doi:10.1038/s41598-022-07212-5

192. Klocke D, Schmitz H. Water as a major modulator of the mechanical properties of insect cuticle. *Acta Biomater*. 2011;7(7). doi:10.1016/j.actbio.2011.04.004

193. Work RW. Dimensions, Birefringences, and Force-Elongation Behavior of Major and Minor Ampullate Silk Fibers from Orb-Web-Spinning Spiders—The Effects of Wetting on these Properties. *Text Res J*. 1977;47(10). doi:10.1177/004051757704701003

194. Polis GA. *The Biology of Scorpions*. Stanford, CA: Stanford University Press; 1990.

195. Droogendijk H, De Boer MJ, Sanders RGP, Krijnen GJM. A biomimetic accelerometer inspired by the cricket's clavate hair. *J R Soc Interface*. 2014;11(97). doi:10.1098/rsif.2014.0438

196. Fan Z, Chen J, Zou J, Bullen D, Liu C, Delcomyn F. Design and fabrication of artificial lateral line flow sensors. *J Micromechanics Microengineering*. 2002;12(5). doi:10.1088/0960-1317/12/5/322

197. Au WWL. Echolocation signals of wild dolphins. *Acoust Phys*. 2004;50(4). doi:10.1134/1.1776224

198. Nihoul JCJ. Echolocation in Bats and Dolphins. *J Mar Syst*. 2004;50(3-4). doi:10.1016/j.jmarsys.2004.01.009

199. Au WWL. Echolocation in dolphins with a dolphin-bat comparison. *Bioacoustics*. 1997;8(1-2). doi:10.1080/09524622.1997.9753357

200. Melcón, ML, Failla, M, Iñíguez MA. Echolocation behavior of franciscana dolphins (Pontoporia blainvillei) in the wild . *J Acoust Soc Am*. 2012;131(6). doi:10.1121/1.4710837

201. Madsen PT, Lammers M, Wisniewska D, Beedholm K. Nasal sound production in echolocating delphinids (Tursiops truncatus and Pseudorca crassidens) is dynamic, but

unilateral: Clicking on the right side and whistling on the left side. *J Exp Biol*. 2013;216(21). doi:10.1242/jeb.091306

202. Kloepper LN, Nachtigall PE, Donahue MJ, Breese M. Active echolocation beam focusing in the false killer whale, Pseudorca crassidens. *J Exp Biol*. 2012;215(8). doi:10.1242/jeb.066605

203. Hemilä S, Nummela S, Reuter T. Anatomy and physics of the exceptional sensitivity of dolphin hearing (Odontoceti: Cetacea). *J Comp Physiol A Neuroethol Sensory, Neural, Behav Physiol*. 2010;196(3). doi:10.1007/s00359-010-0504-x

204. Thewissen JGM, Hussain ST. Origin of underwater hearing in whales. *Nature*. 1993;361(6411). doi:10.1038/361444a0

205. Cranford TW, Krysl P, Hildebrand JA. Acoustic pathways revealed: Simulated sound transmission and reception in Cuvier's beaked whale (Ziphius cavirostris). *Bioinspiration and Biomimetics*. 2008;3(1). doi:10.1088/1748-3182/3/1/016001

206. Wei C, Hoffmann-Kuhnt M, Au WWL, et al. Possible limitations of dolphin echolocation: a simulation study based on a cross-modal matching experiment. *Sci Rep*. 2021;11(1). doi:10.1038/s41598-021-85063-2

207. Dible SA, Flint JA, Lepper PA. On the role of periodic structures in the lower jaw of the atlantic bottlenose dolphin (Tursiops truncatus). *Bioinspiration and Biomimetics*. 2009;4(1). doi:10.1088/1748-3182/4/1/015005

208. Norris KS, Mohl B. Can odontocetes debilitate prey with sound? *Am Nat*. 1983;122(1). doi:10.1086/284120

209. Benoit-Bird KJ, Au WWL, Kastelein R. Testing the odontocete acoustic prey debilitation hypothesis: No stunning results. *J Acoust Soc Am*. 2006;120(2). doi:10.1121/1.2211508

210. Au WWL, Benoit-Bird KJ. Automatic gain control in the echolocation system of

dolphins. *Nature*. 2003;423(6942). doi:10.1038/nature01727

211. Nachtigall PE, Supin AY. A false killer whale adjusts its hearing when it echolocates. *J Exp Biol*. 2008;211(11). doi:10.1242/jeb.013862

212. Parsons ECM. Impacts of Navy sonar on whales and dolphins: Now beyond a smoking gun? *Front Mar Sci*. 2017;4(SEP). doi:10.3389/fmars.2017.00295

213. Reinwald M, Grimal Q, Marchal J, Catheline S, Boschi L. Bone-conducted sound in a dolphin's mandible: Experimental investigation of elastic waves mediating information on sound source position. *J Acoust Soc Am*. 2018;144(4). doi:10.1121/1.5063356

214. Cranford TW, Amundin M, Norris KS. Functional morphology and homology in the odontocete nasal complex: Implications for sound generation. *J Morphol*. 1996;228(3). doi:10.1002/(SICI)1097-4687(199606)228:3<223::AID-JMOR1>3.0.CO;2-3

215. Jakobsen L, Christensen-Dalsgaard J, Juhl PM, Elemans CPH. How Loud Can you go? Physical and Physiological Constraints to Producing High Sound Pressures in Animal Vocalizations. *Front Ecol Evol*. 2021;9. doi:10.3389/fevo.2021.657254

216. Rand AS, Dudley R. Frogs in Helium: The Anuran Vocal Sac Is Not a Cavity Resonator. *Physiol Zool*. 1993;66(5). doi:10.1086/physzool.66.5.30163824

217. Riede T, Beckers GJL, Blevins W, Suthers RA. Inflation of the esophagus and vocal tract filtering in ring doves. *J Exp Biol*. 2004;207(23). doi:10.1242/jeb.01256

218. Dunn JC, Halenar LB, Davies TG, et al. Evolutionary trade-off between vocal tract and testes dimensions in howler monkeys. *Curr Biol*. 2015;25(21). doi:10.1016/j.cub.2015.09.029

219. Veselka N, McErlain DD, Holdsworth DW, et al. A bony connection signals laryngeal echolocation in bats. *Nature*. 2010;463(7283). doi:10.1038/nature08737

220. Mhatre N, Malkin R, Deb R, Balakrishnan R, Robert D. Tree crickets optimize the acoustics of baffles to exaggerate their mate-attraction signal. *Elife*. 2017;6.

doi:10.7554/eLife.32763.001

221. Da Cunha RGT, Byrne RW. Roars of black howler monkeys (Alouatta caraya): Evidence for a function in inter-group spacing. *Behaviour*. 2006;143(10). doi:10.1163/156853906778691568

222. Riede T, Tokuda IT, Munger JB, Thomson SL. Mammalian laryngseal air sacs add variability to the vocal tract impedance: Physical and computational modeling. *J Acoust Soc Am*. 2008;124(1). doi:10.1121/1.2924125

223. Schön Ybarra M. Morphological adaptations for loud phonation in the vocal organ of howling monkeys. *Primate Rep*. 1988;22(1).

224. Fitch WT, Hauser MD. Vocal production in nonhuman primates: Acoustics, physiology, and functional constraints on "honest" advertisement. *Am J Primatol*. 1995;37(3). doi:10.1002/ajp.1350370303

225. Haimoff EH. Brief report: Occurrence of anti-resonance in the song of the siamang (Hylobates syndactylus). *Am J Primatol*. 1983;5(3). doi:10.1002/ajp.1350050309

226. Robles L, Ruggero MA. Mechanics of the mammalian cochlea. *Physiol Rev*. 2001;81(3). doi:10.1152/physrev.2001.81.3.1305

227. Reichenbach T, Hudspeth AJ. The physics of hearing: Fluid mechanics and the active process of the inner ear. *Reports Prog Phys*. 2014;77(7). doi:10.1088/0034-4885/77/7/076601

228. von Békésy G, Peake WT. Experiments in Hearing . *J Acoust Soc Am*. 1990;88(6). doi:10.1121/1.399656

229. Emadi G, Richter CP, Dallos P. Stiffness of the Gerbil Basilar Membrane: Radial and Longitudinal Variations. *J Neurophysiol*. 2004;91(1). doi:10.1152/jn.00446.2003

230. W. LR. The Theory of Sound. *Nature*. 1898;58(1493). doi:10.1038/058121a0

231. Eguíluz VM, Ospeck M, Choe Y, Hudspeth AJ, Magnasco MO. Essential

nonlinearities in hearing. *Phys Rev Lett*. 2000;84(22). doi:10.1103/PhysRevLett.84.5232

232. Hudspeth AJ, Jülicher F, Martin P. A critique of the critical cochlea: Hopf - A bifurcation - Is better than none. *J Neurophysiol*. 2010;104(3). doi:10.1152/jn.00437.2010

233. Kemp DT. Evidence of mechanical nonlinearity and frequency selective wave amplification in the cochlea. *Arch Otorhinolaryngol*. 1979;224(1-2). doi:10.1007/BF00455222

234. Ruggero MA, Rich NC, Recio A. The effect of intense acoustic stimulation on basilar-membrane vibrations. *Audit Neurosci*. 1996;2(4).

235. Ren T, He W, Gillespie PG. Measurement of cochlear power gain in the sensitive gerbil ear. *Nat Commun*. 2011;2(1). doi:10.1038/ncomms1226

236. De Boer E. Mechanics of the Cochlea: Modeling Efforts. In: ; 1996. doi:10.1007/978-1-4612-0757-3_5

237. Ni G, Elliott SJ, Ayat M, Teal PD. Modelling cochlear mechanics. *Biomed Res Int*. 2014;2014. doi:10.1155/2014/150637

238. Manoussaki D, Dimitriadis EK, Chadwick RS. Cochlea's graded curvature effect on low frequency waves. *Phys Rev Lett*. 2006;96(8). doi:10.1103/PhysRevLett.96.088701

239. Manoussaki D, Chadwick RS, Ketten DR, Arruda J, Dimitriadis EK, O'Malley JT. The influence of cochlear shape on low-frequency hearing. *Proc Natl Acad Sci U S A*. 2008;105(16). doi:10.1073/pnas.0710037105

240. Rupin M, Lerosey G, De Rosny J, Lemoult F. Mimicking the cochlea with an active acoustic metamaterial. *New J Phys*. 2019;21(9). doi:10.1088/1367-2630/ab3d8f

241. Fettiplace R, Nam JH. Tonotopy in calcium homeostasis and vulnerability of cochlear hair cells. *Hear Res*. 2019;376. doi:10.1016/j.heares.2018.11.002

242. Ma F, Wu JH, Huang M, Fu G, Bai C. Cochlear bionic acoustic metamaterials. *Appl Phys Lett*. 2014;105(21). doi:10.1063/1.4902869

243. Zhao L, Zhou S. Compact acoustic rainbow trapping in a bioinspired spiral array of graded locally resonant metamaterials. *Sensors (Switzerland)*. 2019;19(4). doi:10.3390/s19040788

244. Karlos A, Elliott SJ. Cochlea-inspired design of an acoustic rainbow sensor with a smoothly varying frequency response. *Sci Rep*. 2020;10(1). doi:10.1038/s41598-020-67608-z

245. Gu GX, Dimas L, Qin Z, Buehler MJ. Optimization of Composite Fracture Properties: Method, Validation, and Applications. *J Appl Mech Trans ASME*. 2016;83(7). doi:10.1115/1.4033381

246. Diaz AR, Haddow AG, Ma L. Design of band-gap grid structures. *Struct Multidiscip Optim*. 2005;29(6). doi:10.1007/s00158-004-0497-6

247. Halkjær S, Sigmund O, Jensen JS. Inverse design of phononic crystals by topology optimization. *Zeitschrift fur Krist*. 2005;220(9-10). doi:10.1524/zkri.2005.220.9-10.895

248. Hedayatrasa S, Abhary K, Uddin M. Numerical study and topology optimization of 1D periodic bimaterial phononic crystal plates for bandgaps of low order Lamb waves. *Ultrasonics*. 2015;57(C). doi:10.1016/j.ultras.2014.11.001

249. Chen Y, Huang X, Sun G, Yan X, Li G. Maximizing spatial decay of evanescent waves in phononic crystals by topology optimization. *Comput Struct*. 2017;182. doi:10.1016/j.compstruc.2017.01.001

250. Wilm M, Ballandras S, Laude V, Pastureaud T. A full 3D plane-wave-expansion model for 1-3 piezoelectric composite structures. *J Acoust Soc Am*. 2002;112(3). doi:10.1121/1.1496081

1475 251. Mace BR, Manconi E. Modelling wave propagation in two-dimensional structures
1476 using finite element analysis. *J Sound Vib*. 2008;318(4-5).
1477 doi:10.1016/j.jsv.2008.04.039
1478 252. Kafesaki M, Economou EN. Multiple-scattering theory for three-dimensional periodic
1479 acoustic composites. *Phys Rev B - Condens Matter Mater Phys*. 1999;60(17).
1480 doi:10.1103/PhysRevB.60.11993
1481 253. Xie L, Xia B, Liu J, Huang G, Lei J. An improved fast plane wave expansion method
1482 for topology optimization of phononic crystals. *Int J Mech Sci*. 2017;120.
1483 doi:10.1016/j.ijmecsci.2016.11.023
1484 254. D'Alessandro L, Bahr B, Daniel L, Weinstein D, Ardito R. Shape optimization of
1485 solid–air porous phononic crystal slabs with widest full 3D bandgap for in-plane
1486 acoustic waves. *J Comput Phys*. 2017;344. doi:10.1016/j.jcp.2017.05.018
1487 255. Costagliola G, Guarino R, Bosia F, Gkagkas K, Pugno NM. Evolutionary Algorithm
1488 Optimization of Staggered Biological or Biomimetic Composites Using the Random
1489 Fuse Model. *Phys Rev Appl*. 2020;13(3). doi:10.1103/PhysRevApplied.13.034049
1490 256. Han XK, Zhang Z. Topological Optimization of Phononic Crystal Thin Plate by a
1491 Genetic Algorithm. *Sci Rep*. 2019;9(1). doi:10.1038/s41598-019-44850-8
1492 257. Liu R, Kumar A, Chen Z, Agrawal A, Sundararaghavan V, Choudhary A. A predictive
1493 machine learning approach for microstructure optimization and materials design. *Sci*
1494 *Rep*. 2015;5. doi:10.1038/srep11551
1495 258. Jin Y, He L, Wen Z, et al. Intelligent on-demand design of phononic metamaterials.
1496 *Nanophotonics*. 2022;11(3). doi:10.1515/nanoph-2021-0639
1497 259. Chatterjee T, Chakraborty S, Goswami S, Adhikari S, Friswell MI. Robust topological
1498 designs for extreme metamaterial micro-structures. *Sci Rep*. 2021;11(1).
1499 doi:10.1038/s41598-021-94520-x

260. Zhang H, Luo Y, Kang Z. Bi-material microstructural design of chiral auxetic metamaterials using topology optimization. *Compos Struct*. 2018;195. doi:10.1016/j.compstruct.2018.04.058

261. Edmunds M. *Defense in Animals: A Survey of Anti-Predator Defenses*. Longman; 1974.

Figure titles and legends

Figure 1:Mantis shrimp

a) Peacock mantis shrimp, with highlighted raptorial dactyl clubs to strike hard objects (adapted from [18]); b) Morphological features of the clubs, in cross-section view, divided in an impact region, a periodic region and a striated region; c) Scanning electron micrograph of the coronal cross-section, showing reinforcing fibre helicoidal arrangement; d) schematic of a Finite Element Analysis model accounting for graded material properties (adapted from [19]).

Figure 2: Vibration attenuation in the woodpecker skull (adapted from [31])

(A): Volume fraction ratio of skull bone, local measured modulus, and macro-equivalent modulus around the skull. (B): 3D finite-element model of the skull and hyoid bone. Note that the Young's modulus on the skull is not uniform. (C): first ten modes of the skull under a pre-tension on the hyoid in the range 0-25 N. (D), upper panel: stress wave at a brain location under impact direction. (d), lower panel: stress spectrum in the frequency domain obtained by FFT.

Figure 3: Modelling of vibration attenuation in the woodpecker skull (adapted from [10])

(A): lumped-elements model of the head of a woodpecker. (B): empirical model of the spongy bone by means of an aluminium enclosure filled with glass microspheres. (C): vibration transmissibility as a function of frequency for different diameters of the SiO2 microspheres.

Figure 4: Biological systems with suture tessellation

(a) examples from Flora and Fauna (adapted from [58]); (b) the leatherback turtle shell (adapted from [60])

Figure 5: Prey sensing similarities in spiders and scorpions

a) web structure: a typical orb web of a spider Nuctenea umbratica. The web is built by means of junctions between threads and surfaces, b) junctions between radial threads, c) and junctions between radial and spiral threads. A flying prey can be eventually detected by air flow sensors, d) the tricobothria. If the prey impacts the web, the vibrational signal will be transmitted mainly by radial threads and be perceived by e) lyriform organs of the spider. Figure adapted from [93,132]. f) schematic of scorpion prey detection using surface waves; g) sensory hairs and mechanoreceptors located at the slit sensilla sense surface waves. Adapted from [162159]

Figure 6: Anti-predatory strategies

(a) The high-resolution 3D acoustic imaging system evolved by the echolocating bats (adapted from [174]) and the moth's strategies to avoid being detected: (b) appropriate scale arrangement and structure (adapted from [178]). and (c) hindwing tails. Behavioural analyses reveal that (A) bats aim an increasing proportion of their attacks at the posterior half of the moth (indicated by yellow cylinder with asterisk) and that (B) bats attacked the first and third sections of tailed moths 75% of the time, providing support for the multiple-target illusion. An enlarged echo illusion would likely lead bats to target the hindwing just behind the abdomen of the moth, at the perceived echo center (highlighted in green); however, bats targeted this region only 25% of the time (adapted from ([261]).

Figure 7: Tiling patterns and acoustic effects of lepidopteran scales

(a) SEM images of butterflies Graphium agamemnon and Danaus chrysippus and moths Dactyloceras lucina and Antheraea pernyi, (b) Change in target strength caused by presence of scales, and equivalent intensity absorption coefficient, (c) Change in target strength caused

by presence of scales, and equivalent absorption coefficient as a function of wing thickness/wavelength. (Adapted from[185])

Figure 8: Sound generation in Howler monkeys

a) The exceptionally low frequency of Howler Monkey vocalizations; b) Howler Monkey vocal apparatus. Adapted from [218].

Figure 9 : Metamaterial inspired by the cochlea

Some of the examples of cochlea-inspiration for the design of metamaterials. In particular, in panels A,B,C, a gradient-index metamaterial for airborne sounds, made from 38 quarter-wavelength acoustic resonators of different heights is reproduced (adapted from [240]). In panel D, a rainbow trapper based on a set of Helmholtz resonators is described (adapted from [243]). In panel E, a modal analysis of a helix model of cochlea is reported, showing a different response to different frequency excitations.